

1 Development of an Integrated Sample Amplification Control 2 for Salivary Point-of-Care Pathogen Testing

3
4 Navaporn Sritong¹, Winston Wei Ngo¹, Karin F. K. Ejendal¹, Jacqueline C. Linnes^{1,2*}

5 1: Weldon School of Biomedical Engineering, Purdue University, West Lafayette, IN, USA

6 2: Department of Public Health, Purdue University, West Lafayette, IN, USA

7 * jlinnes@purdue.edu, +1-765-409-1012

8 9 **Keywords**

10 Reverse transcription Loop-mediated isothermal amplification, SARS-CoV-2, Diagnostic, Lateral flow
11 immunoassay, Internal amplification control, Saliva

12 13 **Abstract**

14 Background: The COVID-19 pandemic has led to a rise in point-of-care (POC) and home-based tests, but
15 concerns over usability, accuracy, and effectiveness have arisen. The incorporation of internal amplification
16 controls (IACs), essential control for translational POC diagnostics, could mitigate false-negative and false-
17 positive results due to sample matrix interference or inhibition. Although emerging POC nucleic acid
18 amplification tests (NAATs) for detecting SARS-CoV-2 show impressive analytical sensitivity in the lab,
19 the assessment of clinical accuracy with IACs is often overlooked. In some cases, the IACs were run
20 spatially, complicating assay workflow. Therefore, the multiplex assay for pathogen and IAC is needed.

21
22 Results: We developed a one-pot duplex reverse transcriptase loop-mediated isothermal amplification (RT-
23 LAMP) assay for saliva samples, a non-invasive and simple collected specimen for POC NAATs. The
24 ORF1ab gene of SARS-CoV-2 was used as a target and a human 18S ribosomal RNA in human saliva was
25 employed as an IAC to ensure clinical reliability of the RT-LAMP assay. The optimized assay could detect
26 SARS-CoV-2 viral particles down to 100 copies/ μ L of saliva within 30 minutes without RNA extraction.
27 The duplex RT-LAMP for SARS-CoV-2 and IAC is successfully amplified in the same reaction without
28 cross-reactivity. The valid results were easily visualized in triple-line lateral flow immunoassay, in which
29 two lines (flow control and IAC lines) represent valid negative results and three lines (flow control, IAC,
30 and test line) represent valid positive results. This duplex assay demonstrated a clinical sensitivity of 95%,
31 specificity of 100%, and accuracy of 96% in 30 clinical saliva samples.

32
33 Significance: IACs play a crucial role in ensuring user confidence with respect to the accuracy and
34 reliability of at-home and POC molecular diagnostics. We demonstrated the multiplex capability of SARS-
35 COV-2 and human 18S ribosomal RNA RT-LAMP without complicating assay design. This generic platform
36 can be extended in a similar manner to include human 18S ribosomal RNA IACs into different clinical
37 sample matrices.

38
39
40
41
42
43
44
45
46

47 Introduction

48
49 Due to the COVID-19 pandemic, there has been a rapid increase in the development and availability of
50 point-of-care (POC) and home-based nucleic acid amplification tests (NAATs) for respiratory infections.
51 However, this has also given rise to user concerns regarding the accuracy and effectiveness of these tests
52 and has raised questions about the future of at-home diagnostics for other infectious diseases [1]. Without
53 the same level of quality control and assurance as laboratory-based tests, sample quality and the way it is
54 collected and handled can lead to challenges with accuracy, reliability, and reproducibility [2].

55
56 According to the US FDA guidelines for *in vitro* diagnostic devices, internal analytical controls (IACs) are
57 among the essential controls mandated for the industry [3]. In the lab, an IAC is commonly run in parallel
58 with NAATs in order to rule out a false-negative result [4] and to qualify the sample collection process as
59 well as the integrity of the amplification enzymes and conditions in a presence of complex matrix [5]. An
60 IAC, sometimes referred to as a sample adequacy control, can contain a synthetic target sequence of
61 different length, a non-target sequence, or a housekeeping gene of human cells to ensure sample is
62 adequately collected and prepared. IACs are also crucial in POC diagnostics to ensure accurate and reliable
63 detection, particularly when performed at locations with limited access to laboratory facilities [6]. The
64 inclusion of an IAC in POC diagnostics can help to reduce the risk of false-negative results, which can have
65 serious implications for the management of infectious diseases due to delayed or inadequate treatment,
66 potentially resulting in disease transmission, increased morbidity, and mortality [7].

67
68 While many emerging publications on NAATs for SARS-CoV-2 show remarkable analytical sensitivity in
69 the laboratory setting [8], assessing clinical accuracy with IAC is often overlooked. Incorporating an IAC
70 into POC NAATs can present challenges such as requirements of more complex assay design and higher
71 volume of samples to run the control, which subsequently leads to additional user step. Nevertheless, there
72 are some works that have integrated an IAC on their diagnostic assays as shown in Table 1. Reported IACs
73 were performed in separated reactions from tests for the virus, leading additional user steps, increased cost
74 of reagents, and increased risk of contamination between samples [9–15]. In contrast, a one-pot multiplexed
75 reaction can streamline the assay workflow, decrease the required sample volume, and mitigate the
76 likelihood of cross-contamination among reaction zones, leading to enhanced assay efficacy [16]. While
77 details are not stated, some portable and benchtop commercial SARS-CoV-2 molecular diagnostic tests
78 such as ID NOW™ COVID-19 2.0, Visby Medical Respiratory Health Test, Aptitude Metrix™ COVID-
79 19 test, and Cue’s COVID-19 Diagnostic Test included IAC in their tests as part of result interpretation
80 [17].

81
82 Isothermal amplification reactions, such as reverse transcription loop-mediated isothermal amplification
83 (RT-LAMP) for the detection of SARS-CoV-2 have recently been highlighted due to their key features:
84 rapid detection without the need for sophisticated equipment or specialized training [18], reagent
85 accessibility [19], comparable sensitivity and specificity [20]. With 6 separate primers required,
86 multiplexed RT-LAMP are commonly not considered. However, multiple publications have demonstrated
87 that RT-LAMP assays can be multiplexed to detect multiple targets in a single reaction [21–23]. These can
88 be achieved by including multiple primer sets targeting different regions of the target sequence, as well as
89 incorporating separate probes to differentiate the amplified products.

90
91 Choosing an appropriate sample matrix for viral infection diagnosis is essential as it plays a key role in
92 obtaining reliable diagnostic results. Saliva has been reported as an alternative to nasopharyngeal specimens
93 for respiratory virus testing including SARS-CoV-2 [24]. Overall, saliva sampling offers several advantages
94 in terms of simplicity for users. Saliva collection is user-friendly and can be performed without medical
95 personnel, reducing the burden on healthcare professionals. Due to its non-invasive nature, saliva sampling
96 is less intimidating, especially for children and older individuals who may have difficulty with nasal swab

97 collection [25]. Moreover, the time required for specimen collection and the associated cost of using saliva
98 are significantly lower compared to using nasopharyngeal specimens [26].

99
100 Despite being easier to collect, salivary components have been demonstrated to hinder RT-LAMP reactions,
101 posing similar challenges to those observed with nasal swab samples. As a result, false-negative results due
102 to assay failure could be observed. To improve clinical accuracy and ease of use and avoiding the drawbacks
103 of a parallel reaction, we have developed a one-pot duplex RT-LAMP assay that uses human 18S ribosomal
104 RNA (18S rRNA) as an IAC in human saliva with the ORF1ab gene of SARS-CoV-2 as the target pathogen.
105 Our optimized assay can detect SARS-CoV-2 viral particles as low as 100 copies/ μ L of saliva within 30
106 minutes. The duplex RT-LAMP for SARS-CoV-2 and IAC can be amplified in one-pot reactions without
107 cross-reactivity, and valid results are easily visualized in triple-line lateral flow immunoassays (LFIA).
108 The appearance of flow control and IAC lines represent valid negative results, and the flow control, IAC,
109 and test lines represent valid positive results. The duplex RT-LAMP assay was validated directly on clinical
110 saliva samples without prior RNA extraction. The IAC developed here meet the FDA guidelines for *In*
111 *Vitro* Diagnostic Devices [6] to bring clinically relevant molecular diagnostic into POC settings without
112 complicating platform design.

113 114 **2. Materials and methods**

115 116 *2.1 Reagents*

117
118 Reagents for RT-LAMP reactions included WarmStart® Multi-Purpose LAMP/RT-LAMP 2X Master Mix
119 with UDG from NEB (Ipswich, MA), EvaGreen from VWR International (Radnor, PA), ROX from Thermo
120 Fisher Scientific (Waltham, MA), and nuclease-free water from Invitrogen (Waltham, MA). Pooled human
121 saliva used in assay development was purchased from Innovative Research (Novi, MI). BtsYI and Ddel
122 restriction enzymes were purchased from NEB (Ipswich, MA). The viral templates obtained from BEI
123 Resources (Manassas, VA) included Heat inactivated Novel Coronavirus, 2019-nCoV/USA-WA1/2020,
124 NR-52286 (SARS-CoV-2); Middle East Respiratory Syndrome Coronavirus (MERS CoV), EMC/2012,
125 Irradiated Infected Cell Lysate, NR-50549; and SARS Coronavirus (SARS), NR-9547; and purified
126 genomic RNA from dengue virus (DENV) type 1. All primers, including those conjugated to FITC, biotin
127 and DIG, were ordered from Integrated DNA Technologies (Coralville, IA).

128 129 *2.2 Singleplex RT-LAMP for SARS-CoV-2 detection*

130
131 The primer set targeting ORF1ab region of SARS-CoV-2 (GenBank: OQ691200.1) was used (Table S1).
132 The RT-LAMP reactions were carried out by using 2x WarmStart® Multi-Purpose LAMP/RT-LAMP
133 Master Mix in accordance with the New England Biolab standard and 10X Primer Mix containing all 6
134 LAMP primers (final concentration of 1.6 μ M for forward inner primer (FIP) and backward inner primer
135 (BIP), 0.4 μ M for forward loop primer (LF) and backward loop primer (LB), and 0.2 μ M for forward outer
136 primer (F3) and backward outer primer (B3). The 5' end of LF and LB were labeled with fluorescein (FITC)
137 or biotin, respectively for LFIA detection. The robustness of primer sets in various saliva percentages (0-
138 30%) were evaluated to determine volume of saliva sample used in the assay. Various concentrations of
139 SARS-CoV-2 viral particles were spiked into saliva samples at concentrations ranging from 0 to 5000
140 SARS-CoV-2 viral copies/ μ L to determine the limit of detection (LOD) of the assay. The saliva without
141 viral particles was used as a no template control (NTC). Five (5) μ L of saliva sample and 20 μ L of
142 mastermix were incubated at 65°C for 30 minutes in a QuantStudio 5 Real-Time PCR machine
143 (ThermoFisher, Waltham, MA). The specificity of optimized RT-LAMP against other coronaviruses was
144 performed by using SARS, MERS CoV, DENV viruses as targets. To validate the amplification process,
145 real-time fluorescence data of EvaGreen intercalating dye and ROX reference dye were recorded. The RT-
146 LAMP amplicons were visualized via LFIA and confirmed via gel electrophoresis using a 2% agarose gel

147 run at 100 V for 50 minutes, stained with ethidium bromide, and imaged using an ultraviolet light gel
148 imaging system (c400, Azure Biosystems, Dublin, CA).

149

150 *2.3 Singleplex RT-LAMP for human RNA in saliva for amplification control*

151

152 To verify the proper collection of saliva and avoid potential false-negative results due to technical errors,
153 we searched the literature for primer sets targeting ubiquitously expressed genes in human samples. In this
154 work, the primer set targeting human 18S rRNA (GenBank: AL592188.60) developed by Garneret et al
155 [11] was selected (Table S1) since it resulted in consistent results. To confirm that IAC primers are
156 orthogonal to SARS-CoV-2 primers and RNA, *in-silico* PCR validation was carried out using free software
157 – UCSC *In-Silico* PCR [27]. The RT-LAMP of IAC was performed as described in singleplex RT-LAMP
158 for SARS-CoV-2 detection experiment. SARS-CoV-2 spiked water, saliva sample, and total human RNA
159 control (Applied Biosystems, Waltham, MA) were used as a template for RT-LAMP of 18S rRNA. The 5'
160 end of LF and LB were tagged with digoxigenin (DIG) and biotin, respectively for LFIA detection. The
161 amplification was confirmed by gel electrophoresis and the LOD was determined via LFIA. In the LOD
162 experiment, the total human RNA control was 10-fold diluted from 4.4×10^6 copies/ μ L and used as
163 templates.

164

165 *2.4 One-pot duplex RT-LAMP of SARS-CoV-2 and human RNA*

166

167 The optimized duplex RT-LAMP consisted of the two sets of 10x Primer Mix targeting the ORF1ab gene
168 or 18S rRNA in which concentrations of FIP and BIP from both sets were adjusted to 1.0 μ M while the
169 concentrations of F3, B3, LF, and LB from both sets remained the same as in the singleplex RT-LAMP
170 conditions. Templates used in these experiments were one target and two target templates. The one target
171 template included SARS-CoV-2 spiked water and saliva without viral particles, while two target template
172 was SARS-CoV-2 spiked saliva. The nuclease-free water was used as NTC in this experiment. The
173 amplifications of duplex RT-LAMP were visualized on triple-line (FITC, DIG, flow control) LFIA strips.
174 The nuclease-free water was used as the NTC to ensure that there is no contamination or cross-reactivity
175 between two primer sets. To assess the LOD of the duplex RT-LAMP assay, saliva samples were spiked
176 with different concentrations of SARS-CoV-2 viral particles ranging from 0 to 5000 SARS-CoV-2 viral
177 copies/ μ L. The duplex RT-LAMP reactions were prepared in total volume of 50 μ L with 5 μ L of sample
178 and incubated at 65°C for 30 minutes in the QuantStudio5 (Applied biosystems, Waltham, MA).

179

180 *2.5 Restriction enzyme digestion of duplex RT-LAMP products*

181

182 To validate the expected amplification products, the duplex RT-LAMP products were digested with the
183 restriction enzyme BtsYI and Ddel that are specific to the products of SARS-CoV-2 and IAC primers,
184 respectively. To determine restriction enzymes that specifically cut the product of SARS-CoV-2 or 18S
185 rRNA RT-LAMP, and not both, the NEBcutter software was used [28]. The templates used in this
186 experiment included SARS-CoV-2 spiked water as SARS-CoV-2 primer product, SARS-CoV-2 free-saliva
187 as IAC primer product, and SARS-CoV-2 spiked saliva as duplex product. The reaction consisted of 5 μ L
188 of amplicons, 2.5 μ L CutSmart Buffer (NEB, Ipswich, MA), and 1 μ L of restriction enzyme. The nuclease-
189 free water was added to fill up reaction volume to 25 μ L. The reactions were then incubated at 37°C in
190 water bath for 20-30 minutes. The restriction fragments of duplex RT-LAMP products were visualized
191 using ethidium bromide in a 2% agarose gel.

192

193 *2.6 Clinical sample validation*

194

195 The developed assay was validated against frozen clinical saliva samples received from Indiana Biobank
196 (Bloomington, IN). The saliva samples were collected in 2 mL cryovials and stored in -80°C upon arrival
197 in our lab. These samples were assigned as study ID 1-30, aliquoted, and used as templates for the standard

198 RT-qPCR and duplex RT-LAMP. Of 30 clinical samples, three (3) SARS-CoV-2 negative samples had
199 insufficient volume to extract RNA and run both RT-qPCR and duplex RT-LAMP. Therefore, additional 3
200 samples were collected from subjects who were negative for COVID-19 by using RNAPro•SAL™ (Oasis
201 Diagnostics®, Vancouver, WA) in accordance with Purdue University IRB protocol # IRB-2020-968. All
202 clinical samples were heat-inactivated at 95°C for 5 minutes to ensure safety of working conditions in a
203 BSL-2 laboratory [29] and stored at -80°C until use. To validate duplex RT-LAMP against clinical samples,
204 5 or 10 µL of heat-inactivated samples were used as templates with 45 or 40 µL of RT-LAMP master mix
205 as described in one-pot duplex RT-LAMP experiment. Each sample was run in triplicate and visualized on
206 trip-line LFIA. The samples for RT-qPCR were extracted by using the QIAamp Viral RNA Mini Kit
207 (Qiagen, Hilden, Germany) according to manufacturer's protocol. Ten (10) µL of extracted samples was
208 used for RT-qPCR analysis using FDA authorized 2019-nCoV: Real-Time Fluorescent RT-PCR kit (BGI,
209 Shenzhen, China) targeted the ORF1ab gene of SARS-CoV-2 genome and human β-actin gene as the IAC.
210 The RT-qPCR was run twice for each sample. The clinical sensitivity and specificity of duplex RT-LAMP
211 assay were evaluated as followed [30]: Sensitivity = (true positive)/(true positive + false negative);
212 Specificity = (true negative)/(true negative + false positive); Accuracy = (true positive + true negative)/(true
213 positive + true negative + false positive + false negative).

214

215 *2.7 LFIA quantification, statistical analysis, and graphical abstract*

216

217 The LFIA tests were run in triplicates for each experiment. The LFIA quantification and statistical analysis
218 were performed as described by Phillips et al [31]. Briefly, after 15 mins of initial sample addition, the
219 LFIAs were scanned using Epson V850 Pro Scanner. A custom MATLAB script was used to quantify the
220 test band, which averages the grey-scale pixel intensity of the test band and subtracts the average
221 background pixel intensity 40 pixels below the test band. The LOD was determined by a one-way ANOVA
222 with Dunnett's *post hoc* test with multiple comparisons using GraphPad prism (GraphPad Software, Boston,
223 MA) of the LFIA test bands of each concentration against the test bands from negative controls (no
224 template) with a 95% confidence interval. The graphical abstract is created in Biorender (Toronto, Canada).

225

226 **3. Results and discussion**

227

228 *3.1 Analytical sensitivity and specificity of SARS-CoV-2 RT-LAMP assay in saliva samples*

229

230 Throughout the stages of infection, the viral load can be as low 10³ to 10⁵ copies/mL of saliva sample
231 (equivalent to 1 to 100 copies/µL of saliva) in early stage and spiked to 10⁸ copies/mL (10⁵ copies/µL) in
232 later stage [32]. To evaluate the analytical sensitivity of SARS-CoV-2 RT-LAMP assay, saliva spiked with
233 various concentration of inactivated SARS-CoV-2 particles was used as templates. The time to detection
234 of SARS-CoV-2 in the RT-LAMP assay was displayed as the cycle threshold (Ct) value against various
235 concentrations of SARS-CoV-2. The singleplex RT-LAMP targeting ORF1ab gene was able to detect as
236 few as 100 SARS-CoV-2 viral copies/µL saliva in less than 30 minutes (Figure 1A). The SARS-CoV-2
237 RT-LAMP products visualized by gel electrophoresis were in a ladder-like pattern (Figure 1B), indicating
238 the successful production of the different length concatemers. The conjugation of the backward loop primer
239 to biotin and the forward loop primer to FITC allowed the result to be readout on LFIAs. The test line of
240 saliva samples with SARS-CoV-2 concentration of 100, 500, and 5000 viral copies/µL were observed
241 (Figure 1C). The presence of the flow control line in all samples suggested that the flow of samples on
242 LFIAs was effective. The analytical sensitivity or LOD of the assay was determined by quantifying test
243 band intensity of each concentration. The custom MATLAB script calculates the average gray-scale pixel
244 intensity of the test band and then subtracts the average background pixel intensity located 40 pixels below
245 the test band. As shown in Figure 1D, there is a statistically significant difference in test band intensity of
246 RT-LAMP products from 100-5000 viral copies/µL in saliva as compared to no template control when
247 using a one-way ANOVA with Dunnett's *post hoc*. The analysis of gel electrophoresis and LFIAs suggested
248 that our SARS-CoV-2 RT-LAMP assay exhibit the LOD of 100 viral copies/µL saliva, which is in the range

249 of clinically relevant LOD [32]. Moreover, the developed RT-LAMP assay was specific to SARS-CoV-2
 250 RNA and demonstrated no amplified products in the gel nor test band on LFIA when viral particles from
 251 MERS, DENV1, or CoV were used as a template (Figure S1). Taken together, the RT-LAMP assay in
 252 saliva is both sensitive and specific for SARS-coV-2 detection.
 253

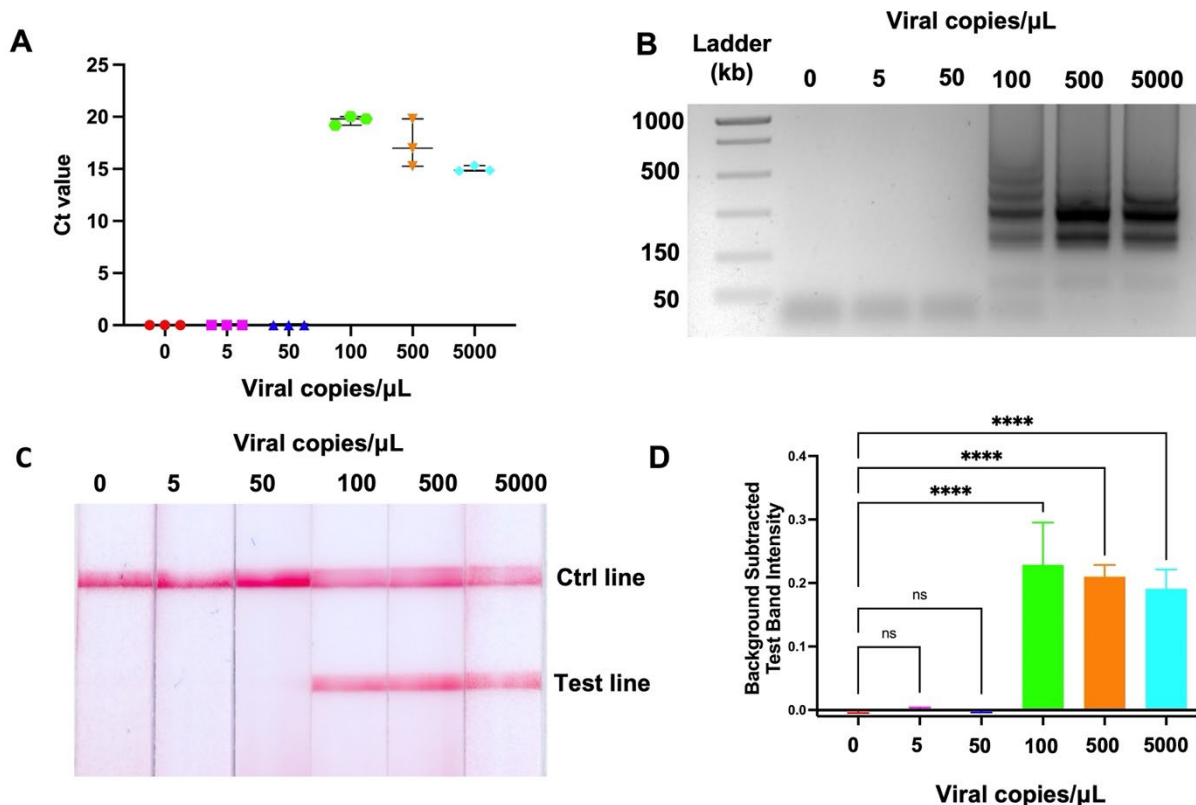


Figure 1. Analytical sensitivity of SARS-CoV-2 RT-LAMP assay in saliva. Ct value of SARS-CoV-2 RT-LAMP in various concentrations (A). RT-LAMP based detection of inactivated viral particles as visualized on gel electrophoresis (B) LFIA (C), and corresponding test band intensity analysis (D). n = 3; **** indicates p value ≤ 0.0001. The ladder-like bands on gel electrophoresis indicating successful amplification.

254

255 3.2 RT-LAMP of 18S ribosomal RNA IAC specific to human RNA in saliva

256

257 IACs are one of the required controls according to the US FDA guideline for *in vitro* diagnostic devices for
 258 various infectious diseases provided to the industry [3]. Given that saliva is the selected sample matrix for
 259 the study, we screened for human genes that are expected to be ubiquitously expressed in human saliva to
 260 use as the IAC target. Regardless of the presence of target pathogen, the IAC should be detectable in all
 261 samples. Another criterion for IAC in this work is that the IAC primers and target should not cross-react
 262 with SARS-CoV-2 primers, or the SAR-CoV-2 target. No matches were found when conducting an *in-*
 263 *silico* analysis of PCR using primers designed for the 18S rRNA against the SARS-CoV-2 genome and
 264 primers (Figure S2). This result suggested that IAC primers are orthogonal to SARS-CoV-2 primers and
 265 RNA. The amplification plot of 18S rRNA RT-LAMP in Figure 2A demonstrates that sigmoidal curve of
 266 the fluorescence signal showed up only when the positive control — total human RNA control and saliva
 267 were used as the templates. The amplicons were subsequently analyzed by the gel electrophoresis. As seen
 268 in Figure 2B, the gel image displayed the ladder-like bandings when total human RNA control and saliva
 269 were used as templates. In contrast, no products were seen on the gel when the template was SARS-CoV-

270 2 particles without saliva. This result confirms that 18S rRNA primers were specific to human RNA control
271 and saliva sample and there is no cross-reactivity against SARS-CoV-2. Therefore, the primer set targeting
272 human 18S rRNA was chosen and incorporated in duplex RT-LAMP as the IAC. It is worth noting that the
273 amount of human 18S rRNA in human saliva can vary depending on several factors including collection
274 method used and the time of day the sample was collected. We ran the LOD of 18S rRNA RT-LAMP and
275 found that the LOD of the assay was 4,400 copies/ μ L (Figure S3), which is in the range of reported
276 concentrations of 18S rRNA in human saliva by other groups [33].

277 In addition to SARS-CoV-2, saliva could serve as specimen for other respiratory viruses [34] such
278 as Influenza viruses, Respiratory Syncytial Virus (RSV), Adenovirus, and Rhinovirus and even bacterial
279 pathogens such as Group A streptococci causing strep throat, and *Bordetella pertussis* causing whooping
280 cough [35]. This study suggests that the 18S rRNA could be a suitable IAC for other diagnostic tests that
281 rely on saliva samples. Moreover, this knowledge could also be similarly employed for integrated IACs in
282 other clinical sample matrixes such as urine, nasal swabs, and blood. Kretschmer-Kazemi Far et al reported
283 that 18S rRNA is the most abundant RNA species in urine samples [36] and Garneret et al. reported the use
284 of 18S rRNA as the IAC for nasal swabs [11]. By performing 18S rRNA RT-LAMP using whole blood
285 (five (5) μ L of undiluted blood), we also demonstrated that 18S rRNA was detectable in freshly collected
286 blood samples (Figure S4.)

287

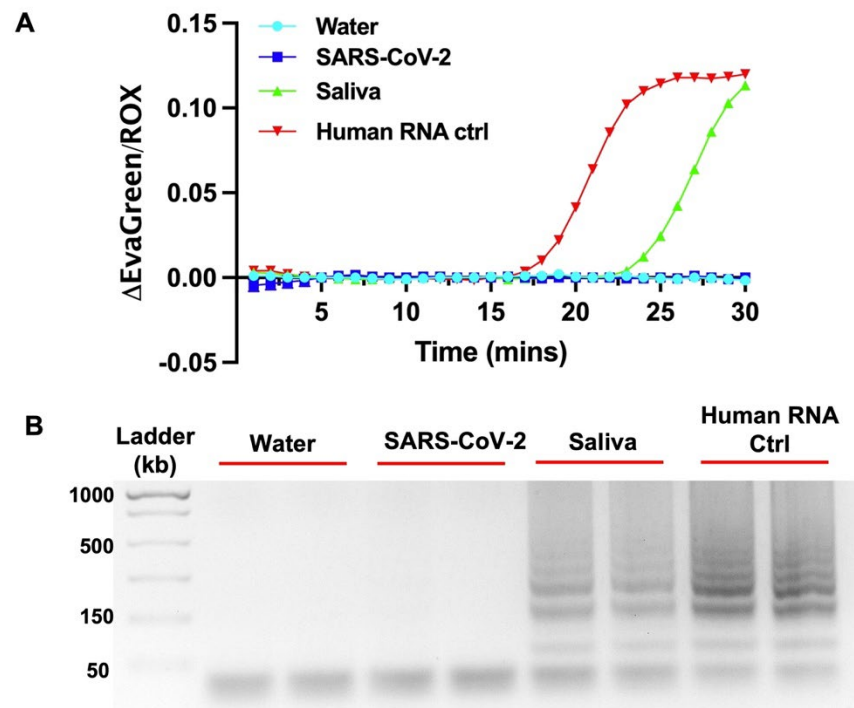


Figure 2. Specificity of IAC primer. Amplification plot (A) and gel electrophoresis (B) of human 18S rRNA RT-LAMP using different templates. The ladder-like bands indicating successful amplification are only present when saliva and human RNA were used as templates. N = 2.

288

289

290 3.3 Optimization of one-pot duplex RT-LAMP of SARS-CoV-2 and IAC

291

292 In general, a one-pot multiplexed reaction can simplify the assay workflow and reduce the amount of sample
293 and reagents required. It can also minimize the risk of cross-contamination between reaction zones and
294 improve the overall assay efficiency. However, a one-pot multiplexed reaction can be more challenging to
295 optimize, and the different targets may compete for limited resources, such as enzymes or primers [37].

296 Therefore, the choices of primers, concentrations, and assay control template are critical to the optimization
 297 process. The duplex RT-LAMP of SARS-CoV-2 and IAC consisting of 2 sets targeting the ORF1ab gene
 298 and 18S rRNA was performed in a single tube “one-pot reaction”. Different template setups were used to
 299 examine the interactions between additional primer sets and their cross-reactivities. The successful
 300 amplification of sample containing one target (SARS-CoV-2 spiked water (W+) and saliva without viral
 301 particles (S-)) and two targets (SARS-CoV-2 spiked saliva (S+)) are shown on the amplification plot (Figure
 302 3A) and gel electrophoresis (Figure 3B). The NTC showed no banding on the gel, confirming that there
 303 was no non-specific amplification or primer-dimers. As seen in Figure 3A, the presence of saliva in SARS-
 304 CoV-2 spiked saliva sample (S+) slowed down the amplification of SARS-CoV-2 primers as compared to
 305 SARS-CoV-2 in water (W+). This is likely due to factors in the complex matrices such as saliva that
 306 interfere with the activity of the enzymes, degrade or inhibit the RNA template or primers, or increase the
 307 viscosity of the reaction mixture [38]. The delayed amplification is not specific to the multiplex RT-LAMP
 308 primer set used here and has been observed before when complex matrices were introduced into LAMP
 309 reaction [39]. The amplicons from different conditions were visualized on a gel were added to LFIA
 310 (Figure 3C). Without templates of both primer sets (NTC) on the W- strip, only the flow control line was
 311 present. As anticipated, the W+ strip showed the flow control and test lines, while the S- strip displayed the
 312 flow control and IAC lines (Figure 3C). The amplicons of both primers were present on the S+ strip,
 313 indicating the successful duplexed RT-LAMP of the target pathogen and IAC in one-pot reaction (n=3).
 314 This duplex reaction demonstrates the multiplexing capabilities of 18S rRNA and the ORF1ab gene of
 315 SARS-CoV-2 in human saliva in the one-pot reaction platform (Figure 3).
 316

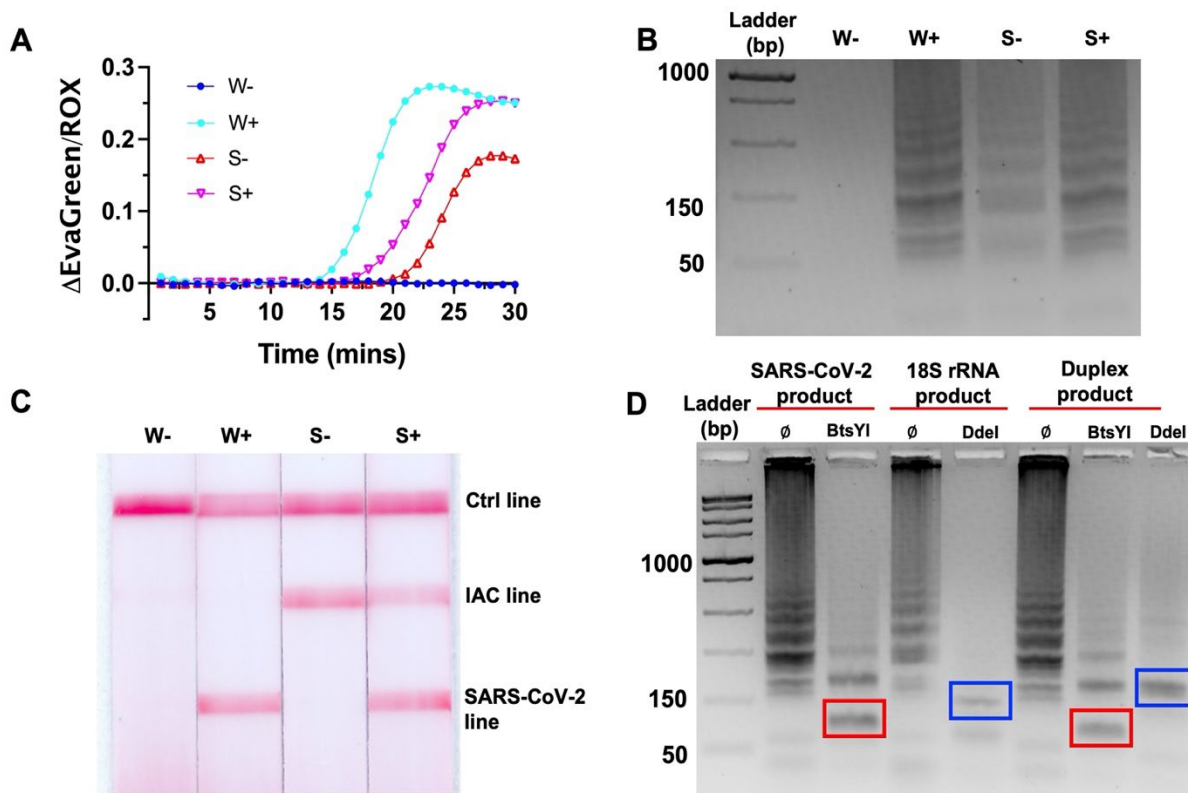


Figure 3. One-pot duplex RT- LAMP of SARS-CoV-2 and human 18S rRNA. (A) Amplification plot of duplex RT-LAMP using different templates. (B) Gel electrophoresis and (C) corresponding LFIA of optimized assay (n=3). Integration of 18S rRNA human sample control into duplex RT-LAMP assay demonstrating differentiation between saliva (with 18S rRNA) and water matrix (without 18S rRNA) and SARS-CoV-2 spiked into each matrix. W- and W+ represent water with and without SARS-CoV-2, respectively. S- and S+ represent saliva sample with and without SARS-CoV-2, respectively. (D)

Restriction enzyme digestion of duplex RT-LAMP of SARS-CoV-2 and human 18S rRNA visualized on the gel. Red boxes indicate BstYI digested amplicon with the characteristic band at 110 bp and blue boxes indicate DdeI digested amplicon the characteristic band at 150 bp. Ø indicate non-digested amplicons.

317

318 *3.4 Validation of the duplex RT-LAMP products by restriction enzyme digestion*

319

320 The amplification products of the two primer sets in the duplex RT-LAMP were also confirmed by
321 restriction enzyme digestion by using two specific restriction enzymes: BtsYI, which targets the product of
322 SARS-CoV-2 primers, and DdeI, which targets the IAC primers (Figure 3D). The digested and non-digested
323 amplicons of SARS-CoV-2, 18S rRNA, and duplex products were shown in Figure 3D. For SARS-CoV-2
324 product (SARS-CoV-2 spiked water), the anticipated 110 bp band was observed after BtsYI digestion as
325 seen in lane 2 on the gel. This band did not show up in non-digested SARS-CoV-2 product in lane 1. In
326 case of 18S rRNA product from saliva without SARS-CoV-2, the characteristic band at approximately 150
327 bp was observed when the amplicons were digested with DdeI as shown in lane 4. In lane 3 of non-digested
328 product, the band at 150 bp was absent. Once the duplex RT-LAMP products from SARS-CoV-2 spiked
329 saliva were digested with BtsYI and DdeI, the characteristic band at 110 bp and 150 bp were visible on the
330 gel in lane 6 and lane 7, respectively, along with smear bands of undigested amplicons. This experiment
331 confirms that the duplex RT-LAMP assay could amplify two targets in the one-pot reaction without cross-
332 reactivity.

333

334 *3.5 Analytical sensitivity of duplex RT-LAMP assay of SARS-CoV-2 and IAC*

335

336 The LOD of the duplex RT-LAMP assay was determined by detecting different concentrations of SARS-
337 CoV-2 spiked into saliva, as was performed in the singleplex SARS-CoV-2 RT-LAMP assay. As seen in
338 Figure 4A, the IAC line showed up in all samples due to the presence of intact human 18S RNA in saliva.
339 The leftmost strip of no viral particles represented a valid negative result. The strips of concentrations
340 ranging from 100-5000 viral copies/ μ L demonstrated 3 lines: flow control, IAC, and SARS-CoV-2 test
341 lines. Figure 4B demonstrates that there is a statistically significantly difference in the test band of duplex
342 RT-LAMP products ranging from 100-5000 viral copies/ μ L compared to no template, as confirmed by a
343 one-way ANOVA with Dunnett's *post hoc* analysis. As a result, the duplex RT-LAMP exhibited a LOD of
344 100 viral copies/ μ L saliva comparable to single plex SARS-CoV-2 RT-LAMP. With prior heat-inactivation
345 of saliva samples, we could bring the LOD down to 50 viral copies/ μ L (Figure S5). Moreover, we found
346 that the IAC line intensity demonstrated a statistically significant decrease as the concentration of SARS-
347 CoV-2 in the sample was increased. On the other hand, the SARS-CoV-2 test line intensity increased in a
348 concentration-dependent manner. Importantly, while the IAC line remained visible in all tests, we
349 hypothesize that in cases of exceptionally high viral loads of SARS-CoV-2, the viral target could
350 outcompete the IAC in samples. This would lead to the absence of IAC at excess SARS-CoV-2
351 concentrations. In this case, users would be informed to interpret any result with a SARS-CoV-2 line as a
352 positive result. The LODs of SARS-CoV-2 RT-LAMP assays can vary depending on several factors such
353 as the type of assay used, the quality of the sample, and the target genes selected for amplification. As
354 compared to several studies that have reported LODs of SARS-Cov-2 ranging from 10 to 1000 viral
355 copies/ μ L [40–43], our duplex RT-LAMP could detect both targets without compromising the sensitivity
356 of SARS-CoV-2 primers.

357

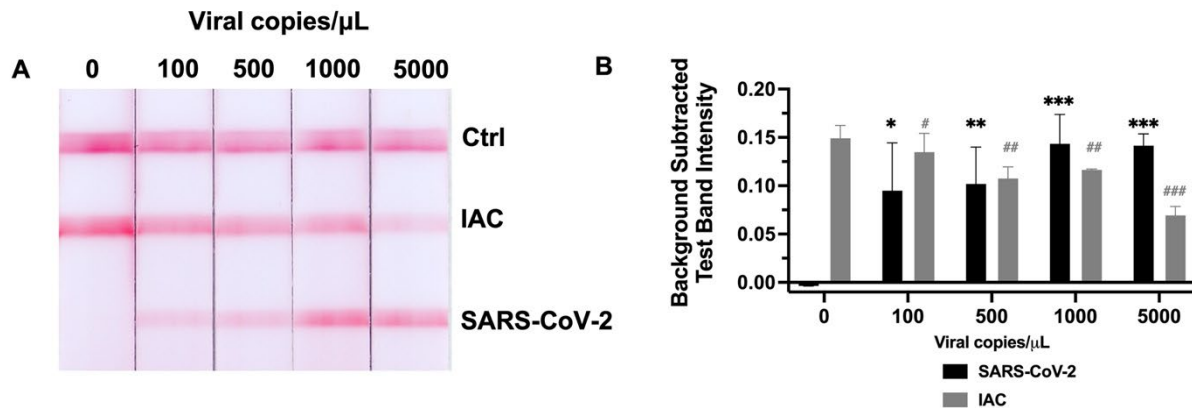


Figure 4. Analytical sensitivity of duplex RT-LAMP assay of SARS-CoV-2 and IAC in saliva visualized on (A) LFIA and (B) corresponding test band intensity analysis. $n = 3$; */# indicates p value ≤ 0.05 ; **/### indicates $p \leq 0.01$; ***/#### indicates p value ≤ 0.001 ; compared to equivalent bands at 0 viral copies/μL.

358

359 3.6 Clinical sample validation

360

361 Clinical sample validation is crucial for the successful implementation of diagnostic assays into clinical
 362 practice. It ensures that the assay is accurate, reliable, and can be used to make informed decisions about
 363 patient care. To evaluate clinical performance of our assay, we tested 30 deidentified clinical samples
 364 received from the Indiana Biobank. Since we intend to implement this assay at point-of-care sites, we
 365 bypassed any RNA extraction steps and validated the duplex assay by using non-extracted samples. The
 366 duplex RT-LAMP assays were run in triplicates for each sample and the results were interpreted on triple-
 367 line LFIA. All LFIA results and quantified test line intensities are shown in Figure S6, Figure S7, and
 368 Table S2. We found that the IAC lines were observed in all samples although the IAC lines of non-extracted
 369 sample ID 10 were faint. Therefore, we ran the assay again with extracted samples and found that the IAC
 370 lines showed up clearly from this extracted sample ID 10 (Figure S5.) and Ct value of 22 obtained from
 371 RT-PCR indicated very high viral load [44]. Saliva sample ID 19 was highly viscous. Therefore, we diluted
 372 this sample with the nuclease-free water in a 1:1 ratio before adding to the reaction. Sample dilution is one
 373 of sample preparation methods for diagnostic tests that has been shown to help reduce inhibitory factors
 374 and viscosity of sample matrices [42].

375

376 The RT-PCR assay of all 30 extracted samples was analyzed as a reference method. The Ct values were
 377 used as a parameter for result interpretation according to manufacture (Table S3). The clinical sensitivity
 378 and specificity of the RT-PCR kit were shown in Table 2. The results suggest that our duplex RT-LAMP
 379 assay with non-extracted samples correctly identified 20 of the 21 RT-PCR-positive samples and accurately
 380 detected all 9 SARS-CoV-2 negative specimens. Only non-extracted sample ID 6 was identified as negative
 381 while the RT-PCR identified as positive. Sample ID 6 had an RT-PCR Ct value of 33, which is considered
 382 to be a very low viral load [45]. When RNA was extracted from sample ID 6, the RT-LAMP assay correctly
 383 identified the sample as positive. In general, the viral load of SARS-CoV-2 in saliva may vary throughout
 384 the different stages of infection. The study conducted by Juanola-Falgarona et al. shows that the viral load
 385 of SARS-CoV-2 in clinical samples exhibited linear relationship with Ct value. The lowest concentration
 386 of $1.00E+02$ copies/mL corresponded to Ct value of 34.9 ± 3 , while the highest concentration of $1.00E+06$
 387 corresponded to Ct value of 23.4 ± 0.7 [46].

388

389 On non-extracted saliva samples, the duplex RT-LAMP achieves 95% clinical sensitivity, 100% clinical
 390 specificity, and 96% accuracy. These are considered well above the acceptable values according to the US
 391 Food and Drug Administration (FDA) guidance for SARS-CoV-2 diagnostic tests Emergency Use
 392 Authorization.

393

Table 2. Calculation of sensitivity and specificity for the Duplex RT-LAMP

		RT-qPCR	
		Positive	negative
Duplex RT-LAMP	positive	20 (TP)	0 (FP)
	negative	1 (FN)	9 (TN)

Sensitivity: 95%

Specificity: 100%

TP: True positive, FP: False positive, FN: False negative, TN: True negative

394

395

4. Conclusion

396

397

398

399

400

401

402

403

404

405

406

407

408

409

We successfully combined an IAC for clinically valid sample collection and assay function with a test for the SARS-CoV-2 virus from saliva using the one-pot duplex RT-LAMP. The test can detect both the target virus (SARS-CoV-2) and IAC in the same reaction without cross-reactivity. Without requiring RNA extraction, the duplex RT-LAMP assay was able to detect SARS-CoV-2 down to 100 copies/ μ L of saliva within 30 minutes, or 50 copies/ μ L with an additional heat inactivation step. The developed assay exhibited 95% clinical sensitivity and 100% specificity with accuracy of 96% on non-extracted saliva samples without heat inactivation. IACs are integral to ensure the accuracy and reliability and user confidence in molecular diagnostics in order to run them at home and at POC sites with minimally trained users. Additionally, both the specific 18S rRNA IAC and general knowledge of duplex RT-LAMP can be applied in similar manner to incorporate IACs into various other clinical sample matrices including blood, urine, and nasal swabs. This work is a promising step toward an integrated sample-to-answer POC device for respiratory infection detection at home or POC sites.

410

CRedit authorship contribution statement

411

412

413

414

415

416

Navaporn Sritong: Conceptualization, Methodology, Investigation, Validation, Writing – original draft
 Winston Wei Ngo: Methodology, Investigation,
 Karin F. K. Ejendal: Methodology, Writing - review & editing.
 Jacqueline C. Linnes: Conceptualization, Writing-review & editing, Supervision, Funding acquisition.

417

Declaration of competing interest

418

419

420

421

422

Jacqueline C. Linnes is co-founder of EverTrue LLC, a diagnostics company developing paper-based POC NAATs, and co-founder of OmniVis Inc. NAAT company developing POC diagnostics. Navaporn Sritong, Winston Wei Ngo, and Karin F. K. Ejendal have declared that they have no competing interests.

423

Acknowledgement

424

425

426

427

428

429

This study received financial support from the Moore Inventor Fellows Award from the Gordon and Betty Moore Foundation Award # 9687 and from NIH National Institute on Drug Abuse award # DP2DA051910. We would like to recognize Dr. Mohit Verma, Assistant Professor in Agricultural and Biological Engineering, Purdue University, for providing information on SARS-CoV-2 primer sequences.

430

Appendix A. Supplementary data

431

432

Data availability

433

434

435

436

No data was used for the research described in the article.

437
438
439
440
441
442
443
444
445
446
447
448
449
450
451
452
453
454
455
456
457
458
459
460
461
462
463
464
465
466
467
468
469
470
471
472
473
474
475
476
477
478
479
480
481
482
483
484
485
486
487

References

- [1] N.V. Tolan, G.L. Horowitz, Clinical Diagnostic Point-of-Care Molecular Assays for SARS-CoV-2, *Clin. Lab. Med.* 42 (2022) 223–236. <https://doi.org/10.1016/j.cll.2022.03.002>.
- [2] J.L.V. Shaw, Practical challenges related to point of care testing, *Pract. Lab. Med.* 4 (2016) 22–29. <https://doi.org/10.1016/j.plabm.2015.12.002>.
- [3] Class II Special Controls Guideline: In Vitro Diagnostic Devices for *Bacillus* spp. Detection, (n.d.).
- [4] K.G. Shah, S. Kumar, P. Yager, Near-digital amplification in paper improves sensitivity and speed in bplexed reactions, *Sci. Rep.* 12 (2022) 14618. <https://doi.org/10.1038/s41598-022-18937-8>.
- [5] C. Schrader, A. Schielke, L. Ellerbroek, R. Johne, PCR inhibitors – occurrence, properties and removal, *J. Appl. Microbiol.* 113 (2012) 1014–1026. <https://doi.org/10.1111/j.1365-2672.2012.05384.x>.
- [6] U.S. Department of Health and Human Services, Food and Drug Administration, Class II Special Controls Guideline: Nucleic Acid Amplification Assays for the Detection of *Trichomonas vaginalis*-Guideline for Industry and Food and Drug Administration Staff, n.d. <https://fda.report/media/92927/Class-II-Special-Controls-Guideline--Nucleic-Acid-Amplification-Assays-for-the-Detection-of-Trichomonas-vaginalis---Guideline-for-Industry-and-Food-and-Drug-Administration-Staff.pdf>.
- [7] S. Garg, L. Kim, M. Whitaker, A. O’Halloran, C. Cummings, R. Holstein, M. Prill, S.J. Chai, P.D. Kirley, N.B. Alden, B. Kawasaki, K. Yousey-Hindes, L. Niccolai, E.J. Anderson, K.P. Openo, A. Weigel, M.L. Monroe, P. Ryan, J. Henderson, S. Kim, K. Como-Sabetti, R. Lynfield, D. Sosin, S. Torres, A. Muse, N.M. Bennett, L. Billing, M. Sutton, N. West, W. Schaffner, H.K. Talbot, C. Aquino, A. George, A. Budd, L. Brammer, G. Langley, A.J. Hall, A. Fry, Hospitalization Rates and Characteristics of Patients Hospitalized with Laboratory-Confirmed Coronavirus Disease 2019 — COVID-NET, 14 States, March 1–30, 2020, *MMWR Morb. Mortal. Wkly. Rep.* 69 (2020) 458–464. <https://doi.org/10.15585/mmwr.mm6915e3>.
- [8] A.D. Subali, L. Wiyono, Reverse Transcriptase Loop Mediated Isothermal Amplification (RT-LAMP) for COVID-19 diagnosis: a systematic review and meta-analysis, *Pathog. Glob. Health.* 115 (n.d.) 281–291. <https://doi.org/10.1080/20477724.2021.1933335>.
- [9] M.N. Anahtar, G.E.G. McGrath, B.A. Rabe, N.A. Tanner, B.A. White, J.K.M. Lennerz, J.A. Branda, C.L. Cepko, E.S. Rosenberg, Clinical Assessment and Validation of a Rapid and Sensitive SARS-CoV-2 Test Using Reverse Transcription Loop-Mediated Isothermal Amplification Without the Need for RNA Extraction, *Open Forum Infect. Dis.* 8 (2021) ofaa631. <https://doi.org/10.1093/ofid/ofaa631>.
- [10] Y. Zhang, G. Ren, J. Buss, A.J. Barry, G.C. Patton, N.A. Tanner, Enhancing colorimetric loop-mediated isothermal amplification speed and sensitivity with guanidine chloride, *BioTechniques.* 69 (2020) 178–185. <https://doi.org/10.2144/btn-2020-0078>.
- [11] P. Garneret, E. Coz, E. Martin, J.-C. Manuguerra, E. Brient-Litzler, V. Enouf, D.F.G. Obando, J.-C. Olivo-Marin, F. Monti, S. van der Werf, J. Vanhomwegen, P. Tabelaing, Performing point-of-care molecular testing for SARS-CoV-2 with RNA extraction and isothermal amplification, *PLOS ONE.* 16 (2021) e0243712. <https://doi.org/10.1371/journal.pone.0243712>.
- [12] G. Papadakis, A.K. Pantazis, N. Fikas, S. Chatziioannidou, V. Tsiakalou, K. Michaelidou, V. Pogka, M. Megariti, M. Vardaki, K. Giarentis, J. Heaney, E. Nastouli, T. Karamitros, A. Mentis, A. Zafiroopoulos, G. Sourvinos, S. Agelaki, E. Gizeli, Portable real-time colorimetric LAMP-device for rapid quantitative detection of nucleic acids in crude samples, *Sci. Rep.* 12 (2022) 3775. <https://doi.org/10.1038/s41598-022-06632-7>.
- [13] B.A. Rabe, C. Cepko, SARS-CoV-2 detection using isothermal amplification and a rapid, inexpensive protocol for sample inactivation and purification, *Proc. Natl. Acad. Sci.* 117 (2020) 24450–24458. <https://doi.org/10.1073/pnas.2011221117>.
- [14] O. Yaren, J. McCarter, N. Phadke, K.M. Bradley, B. Overton, Z. Yang, S. Ranade, K. Patil, R. Bangale, S.A. Benner, Ultra-rapid detection of SARS-CoV-2 in public workspace environments, *PLOS ONE.* 16 (2021) e0240524. <https://doi.org/10.1371/journal.pone.0240524>.

- 488 [15]J.P. Broughton, X. Deng, G. Yu, C.L. Fasching, V. Servellita, J. Singh, X. Miao, J.A. Streithorst, A.
489 Granados, A. Sotomayor-Gonzalez, K. Zorn, A. Gopez, E. Hsu, W. Gu, S. Miller, C.-Y. Pan, H.
490 Guevara, D.A. Wadford, J.S. Chen, C.Y. Chiu, CRISPR–Cas12-based detection of SARS-CoV-2,
491 *Nat. Biotechnol.* 38 (2020) 870–874. <https://doi.org/10.1038/s41587-020-0513-4>.
- 492 [16]S.H. Lee, Y.H. Baek, Y.-H. Kim, Y.-K. Choi, M.-S. Song, J.-Y. Ahn, One-Pot Reverse Transcriptional
493 Loop-Mediated Isothermal Amplification (RT-LAMP) for Detecting MERS-CoV, *Front. Microbiol.*
494 7 (2016) 2166. <https://doi.org/10.3389/fmicb.2016.02166>.
- 495 [17]C. for D. and R. Health, In Vitro Diagnostics EUAs - Molecular Diagnostic Tests for SARS-CoV-2,
496 FDA. (2023). [https://www.fda.gov/medical-devices/covid-19-emergency-use-authorizations-](https://www.fda.gov/medical-devices/covid-19-emergency-use-authorizations-medical-devices/in-vitro-diagnostics-euas-molecular-diagnostic-tests-sars-cov-2)
497 [medical-devices/in-vitro-diagnostics-euas-molecular-diagnostic-tests-sars-cov-2](https://www.fda.gov/medical-devices/in-vitro-diagnostics-euas-molecular-diagnostic-tests-sars-cov-2) (accessed June 5,
498 2023).
- 499 [18]C. Amaral, W. Antunes, E. Moe, A.G. Duarte, L.M.P. Lima, C. Santos, I.L. Gomes, G.S. Afonso, R.
500 Vieira, H.S.S. Teles, M.S. Reis, M.A.R. da Silva, A.M. Henriques, M. Fevereiro, M.R. Ventura, M.
501 Serrano, C. Pimentel, A molecular test based on RT-LAMP for rapid, sensitive and inexpensive
502 colorimetric detection of SARS-CoV-2 in clinical samples, *Sci. Rep.* 11 (2021) 16430.
503 <https://doi.org/10.1038/s41598-021-95799-6>.
- 504 [19]S.A. El-Kafrawy, M.M. El-Daly, A.M. Hassan, S.M. Harakeh, T.A. Alandijany, E.I. Azhar, Rapid and
505 Reliable Detection of SARS-CoV-2 Using Direct RT-LAMP, *Diagnostics.* 12 (2022) 828.
506 <https://doi.org/10.3390/diagnostics12040828>.
- 507 [20]M. Inaba, Y. Higashimoto, Y. Toyama, T. Horiguchi, M. Hibino, M. Iwata, K. Imaizumi, Y. Doi,
508 Diagnostic accuracy of LAMP versus PCR over the course of SARS-CoV-2 infection, *Int. J. Infect.*
509 *Dis.* 107 (2021) 195–200. <https://doi.org/10.1016/j.ijid.2021.04.018>.
- 510 [21]J.H. Kim, M. Kang, E. Park, D.R. Chung, J. Kim, E.S. Hwang, A Simple and Multiplex Loop-Mediated
511 Isothermal Amplification (LAMP) Assay for Rapid Detection of SARS-CoV, *Biochip J.* 13 (2019)
512 341–351. <https://doi.org/10.1007/s13206-019-3404-3>.
- 513 [22]Y. Shao, S. Zhu, C. Jin, F. Chen, Development of multiplex loop-mediated isothermal amplification-
514 RFLP (mLAMP-RFLP) to detect *Salmonella* spp. and *Shigella* spp. in milk, *Int. J. Food Microbiol.*
515 148 (2011) 75–79. <https://doi.org/10.1016/j.ijfoodmicro.2011.05.004>.
- 516 [23]E.C. Kline, N. Panpradist, I.T. Hull, Q. Wang, A.K. Oreskovic, P.D. Han, L.M. Starita, B.R. Lutz,
517 Multiplex Target-Redundant RT-LAMP for Robust Detection of SARS-CoV-2 Using Fluorescent
518 Universal Displacement Probes, *Microbiol. Spectr.* 10 (2022) e01583-21.
519 <https://doi.org/10.1128/spectrum.01583-21>.
- 520 [24]E. Pasomsub, S.P. Watcharananan, K. Boonyawat, P. Janchompoo, G. Wongtabtim, W. Sukswan, S.
521 Sungkanuparph, A. Phuphuakrat, Saliva sample as a non-invasive specimen for the diagnosis of
522 coronavirus disease 2019: a cross-sectional study, *Clin. Microbiol. Infect.* 27 (2021) 285.e1-285.e4.
523 <https://doi.org/10.1016/j.cmi.2020.05.001>.
- 524 [25]A. Langedijk, O. Allicock, M.V. Wijk, D. Yolda-Carr, D. Weinberger, A. Wyllie, L. Bont, Saliva as
525 an alternative to nasopharyngeal swabs for detection of respiratory syncytial virus (RSV) in children,
526 *Eur. Respir. J.* 60 (2022). <https://doi.org/10.1183/13993003.congress-2022.4519>.
- 527 [26]K.K.W. To, C.C.Y. Yip, C.Y.W. Lai, C.K.H. Wong, D.T.Y. Ho, P.K.P. Pang, A.C.K. Ng, K.-H. Leung,
528 R.W.S. Poon, K.-H. Chan, V.C.C. Cheng, I.F.N. Hung, K.-Y. Yuen, Saliva as a diagnostic specimen
529 for testing respiratory virus by a point-of-care molecular assay: a diagnostic validity study, *Clin.*
530 *Microbiol. Infect. Off. Publ. Eur. Soc. Clin. Microbiol. Infect. Dis.* 25 (2019) 372–378.
531 <https://doi.org/10.1016/j.cmi.2018.06.009>.
- 532 [27]L.R. Nassar, G.P. Barber, A. Benet-Pagès, J. Casper, H. Clawson, M. Diekhans, C. Fischer, J.N.
533 Gonzalez, A.S. Hinrichs, B.T. Lee, C.M. Lee, P. Muthuraman, B. Nguy, T. Pereira, P. Nejad, G.
534 Perez, B.J. Raney, D. Schmelter, M.L. Speir, B.D. Wick, A.S. Zweig, D. Haussler, R.M. Kuhn, M.
535 Haeussler, W.J. Kent, The UCSC Genome Browser database: 2023 update, *Nucleic Acids Res.* 51
536 (2023) D1188–D1195. <https://doi.org/10.1093/nar/gkac1072>.
- 537 [28]NEBcutter 3.0, (n.d.). <https://nc3.neb.com/NEBcutter/> (accessed May 25, 2023).

- 538 [29]C. Batéjat, Q. Grassin, J.-C. Manuguerra, I. Leclercq, Heat inactivation of the severe acute respiratory
539 syndrome coronavirus 2, *J. Biosaf. Biosecurity.* 3 (2021) 1–3.
540 <https://doi.org/10.1016/j.jobb.2020.12.001>.
- 541 [30]R. Parikh, A. Mathai, S. Parikh, G. Chandra Sekhar, R. Thomas, Understanding and using sensitivity,
542 specificity and predictive values, *Indian J. Ophthalmol.* 56 (2008) 45–50.
- 543 [31]E.A. Phillips, Stimuli-Responsive Valving Mechanisms for Paper-Based Diagnostics, thesis, Purdue
544 University Graduate School, 2020. <https://doi.org/10.25394/PGS.11949231.v1>.
- 545 [32]E.S. Savela, A. Vilorio Winnett, A.E. Romano, M.K. Porter, N. Shelby, R. Akana, J. Ji, M.M. Cooper,
546 N.W. Schlenker, J.A. Reyes, A.M. Carter, J.T. Barlow, C. Tognazzini, M. Feaster, Y.-Y. Goh, R.F.
547 Ismagilov, Quantitative SARS-CoV-2 Viral-Load Curves in Paired Saliva Samples and Nasal Swabs
548 Inform Appropriate Respiratory Sampling Site and Analytical Test Sensitivity Required for Earliest
549 Viral Detection, *J. Clin. Microbiol.* 60 (2022) e0178521. <https://doi.org/10.1128/JCM.01785-21>.
- 550 [33]P. Ostheim, A. Tichý, I. Sirak, M. Davidkova, M.M. Stastna, G. Kultova, T. Paunesku, G. Woloschak,
551 M. Majewski, M. Port, M. Abend, Overcoming challenges in human saliva gene expression
552 measurements, *Sci. Rep.* 10 (2020) 11147. <https://doi.org/10.1038/s41598-020-67825-6>.
- 553 [34]K.K. To, L. Lu, C.C. Yip, R.W. Poon, A.M. Fung, A. Cheng, D.H. Lui, D.T. Ho, I.F. Hung, K.-H.
554 Chan, K.-Y. Yuen, Additional molecular testing of saliva specimens improves the detection of
555 respiratory viruses, *Emerg. Microbes Infect.* 6 (2017) e49. <https://doi.org/10.1038/emi.2017.35>.
- 556 [35]W. Tu, A.M. McManamen, X. Su, I. Jeacopello, M.G. Takezawa, D.L. Hieber, G.W. Hassan, U.N.
557 Lee, E.V. Anana, M.P. Locknane, M.W. Stephenson, V.A.M. Shinkawa, E.R. Wald, G.P. DeMuri,
558 K.N. Adams, E. Berthier, S. Thongpang, A.B. Theberge, At-Home Saliva Sampling in Healthy Adults
559 Using CandyCollect, a Lollipop-Inspired Device, *Anal. Chem.* 95 (2023) 10211–10220.
560 <https://doi.org/10.1021/acs.analchem.3c00462>.
- 561 [36]R. Kretschmer-Kazemi Far, K. Frank, G. Sczakiel, Sampling, Logistics, and Analytics of Urine for RT-
562 qPCR-based Diagnostics, *Cancers.* 13 (2021) 4381. <https://doi.org/10.3390/cancers13174381>.
- 563 [37]J. Parker, N. Fowler, M.L. Walmsley, T. Schmidt, J. Scharrer, J. Kowaleski, T. Grimes, S. Hoyos, J.
564 Chen, Analytical Sensitivity Comparison between Singleplex Real-Time PCR and a Multiplex PCR
565 Platform for Detecting Respiratory Viruses, *PLOS ONE.* 10 (2015) e0143164.
566 <https://doi.org/10.1371/journal.pone.0143164>.
- 567 [38]Z. Li, J.L. Bruce, B. Cohen, C.V. Cunningham, W.E. Jack, K. Kunin, B.W. Langhorst, J. Miller, R.A.
568 Moncion, C.B. Poole, P.K. Premssirrut, G. Ren, R.J. Roberts, N.A. Tanner, Y. Zhang, C.K.S. Carlow,
569 Development and implementation of a simple and rapid extraction-free saliva SARS-CoV-2 RT-
570 LAMP workflow for workplace surveillance, *PLOS ONE.* 17 (2022) e0268692.
571 <https://doi.org/10.1371/journal.pone.0268692>.
- 572 [39]T.J. Moehling, Portable platforms for molecular-based detection of pathogens in complex sample
573 matrices, thesis, Purdue University Graduate School, 2020.
574 <https://doi.org/10.25394/PGS.12739466.v1>.
- 575 [40]R. Lu, X. Wu, Z. Wan, Y. Li, X. Jin, C. Zhang, A Novel Reverse Transcription Loop-Mediated
576 Isothermal Amplification Method for Rapid Detection of SARS-CoV-2, *Int. J. Mol. Sci.* 21 (2020)
577 2826. <https://doi.org/10.3390/ijms21082826>.
- 578 [41]J. Lim, R. Stavins, V. Kindratenko, J. Baek, L. Wang, K. White, J. Kumar, E. Valera, W.P. King, R.
579 Bashir, Microfluidic point-of-care device for detection of early strains and B.1.1.7 variant of SARS-
580 CoV-2 virus, *Lab. Chip.* 22 (2022) 1297–1309. <https://doi.org/10.1039/D2LC00021K>.
- 581 [42]J.L. Davidson, J. Wang, M.K. Maruthamuthu, A. Dextre, A. Pascual-Garrigos, S. Mohan, S.V.S.
582 Putikam, F.O.I. Osman, D. McChesney, J. Seville, M.S. Verma, A paper-based colorimetric
583 molecular test for SARS-CoV-2 in saliva, *Biosens. Bioelectron.* 9 (2021) 100076.
584 <https://doi.org/10.1016/j.biosx.2021.100076>.
- 585 [43]A.J. Colbert, D.H. Lee, K.N. Clayton, S.T. Wereley, J.C. Linnes, T.L. Kinzer-Ursem, PD-LAMP
586 smartphone detection of SARS-CoV-2 on chip, *Anal. Chim. Acta.* 1203 (2022) 339702.
587 <https://doi.org/10.1016/j.aca.2022.339702>.

- 588 [44]F. Yu, L. Yan, N. Wang, S. Yang, L. Wang, Y. Tang, G. Gao, S. Wang, C. Ma, R. Xie, F. Wang, C.
589 Tan, L. Zhu, Y. Guo, F. Zhang, Quantitative Detection and Viral Load Analysis of SARS-CoV-2 in
590 Infected Patients, *Clin. Infect. Dis. Off. Publ. Infect. Dis. Soc. Am.* 71 (2020) 793–798.
591 <https://doi.org/10.1093/cid/ciaa345>.
- 592 [45]M. Platten, D. Hoffmann, R. Grosser, F. Wisplinghoff, H. Wisplinghoff, G. Wiesmüller, O. Schildgen,
593 V. Schildgen, SARS-CoV-2, CT-Values, and Infectivity—Conclusions to Be Drawn from Side
594 Observations, *Viruses*. 13 (2021) 1459. <https://doi.org/10.3390/v13081459>.
- 595 [46]M. Juanola-Falgarona, L. Peñarrubia, S. Jiménez-Guzmán, R. Porco, C. Congost-Teixidor, M. Varo-
596 Velázquez, S.N. Rao, G. Pueyo, D. Manissero, J. Pareja, Ct values as a diagnostic tool for monitoring
597 SARS-CoV-2 viral load using the QIAstat-Dx® Respiratory SARS-CoV-2 Panel, *Int. J. Infect. Dis.*
598 122 (2022) 930–935. <https://doi.org/10.1016/j.ijid.2022.07.022>.
- 599 [47]B. Bruijns, L. Folkertsma, R. Tiggelaar, FDA authorized molecular point-of-care SARS-CoV-2 tests:
600 A critical review on principles, systems and clinical performances, *Biosens. Bioelectron.* 11 (2022)
601 100158. <https://doi.org/10.1016/j.biosx.2022.100158>.
- 602 [48]G.-S. Park, K. Ku, S.-H. Baek, S.-J. Kim, S.I. Kim, B.-T. Kim, J.-S. Maeng, Development of Reverse
603 Transcription Loop-Mediated Isothermal Amplification Assays Targeting Severe Acute Respiratory
604 Syndrome Coronavirus 2 (SARS-CoV-2), *J. Mol. Diagn. JMD.* 22 (2020) 729–735.
605 <https://doi.org/10.1016/j.jmoldx.2020.03.006>.
- 606 [49]S. Bhadra, T.E. Riedel, S. Lakhotia, N.D. Tran, A.D. Ellington, High-Surety Isothermal Amplification
607 and Detection of SARS-CoV-2, *mSphere*. 6 (2021) e00911-20.
608 <https://doi.org/10.1128/mSphere.00911-20>.
- 609 [50]V.L. Dao Thi, K. Herbst, K. Boerner, M. Meurer, L.P. Kremer, D. Kirrmaier, A. Freistaedter, D.
610 Papagiannidis, C. Galmozzi, M.L. Stanifer, S. Boulant, S. Klein, P. Chlanda, D. Khalid, I. Barreto
611 Miranda, P. Schnitzler, H.-G. Kräusslich, M. Knop, S. Anders, A colorimetric RT-LAMP assay and
612 LAMP-sequencing for detecting SARS-CoV-2 RNA in clinical samples, *Sci. Transl. Med.* 12 (2020)
613 eabc7075. <https://doi.org/10.1126/scitranslmed.abc7075>.
- 614 [51]J. Qian, S.A. Boswell, C. Chidley, Z. Lu, M.E. Pettit, B.L. Gaudio, J.M. Fajnzylber, R.T. Ingram, R.H.
615 Ward, J.Z. Li, M. Springer, An enhanced isothermal amplification assay for viral detection, *Nat.*
616 *Commun.* 11 (2020) 5920. <https://doi.org/10.1038/s41467-020-19258-y>.
- 617 [52]Y.H. Baek, J. Um, K.J.C. Antigua, J.-H. Park, Y. Kim, S. Oh, Y.-I. Kim, W.-S. Choi, S.G. Kim, J.H.
618 Jeong, B.S. Chin, H.D.G. Nicolas, J.-Y. Ahn, K.S. Shin, Y.K. Choi, J.-S. Park, M.-S. Song,
619 Development of a reverse transcription-loop-mediated isothermal amplification as a rapid early-
620 detection method for novel SARS-CoV-2, *Emerg. Microbes Infect.* 9 (2020) 998–1007.
621 <https://doi.org/10.1080/22221751.2020.1756698>.
- 622 [53]C. Yan, J. Cui, L. Huang, B. Du, L. Chen, G. Xue, S. Li, W. Zhang, L. Zhao, Y. Sun, H. Yao, N. Li,
623 H. Zhao, Y. Feng, S. Liu, Q. Zhang, D. Liu, J. Yuan, Rapid and visual detection of 2019 novel
624 coronavirus (SARS-CoV-2) by a reverse transcription loop-mediated isothermal amplification assay,
625 *Clin. Microbiol. Infect. Off. Publ. Eur. Soc. Clin. Microbiol. Infect. Dis.* 26 (2020) 773–779.
626 <https://doi.org/10.1016/j.cmi.2020.04.001>.
- 627 [54]T. Zheng, X. Li, Y. Si, M. Wang, Y. Zhou, Y. Yang, N. Liang, B. Ying, P. Wu, Specific lateral flow
628 detection of isothermal nucleic acid amplicons for accurate point-of-care testing, *Biosens.*
629 *Bioelectron.* 222 (2023) 114989. <https://doi.org/10.1016/j.bios.2022.114989>.
- 630 [55]C. Zhang, J. Lv, Y. Cao, X. Yao, M. Yin, S. Li, J. Zheng, H. Liu, A triple-target reverse transcription
631 loop-mediated isothermal amplification (RT-LAMP) for rapid and accurate detection of SARS-CoV-
632 2 virus, *Anal. Chim. Acta.* 1255 (2023) 341146. <https://doi.org/10.1016/j.aca.2023.341146>.
- 633 [56]P. Nuchnoi, P. Piromtong, S. Siribal, K. Anansilp, P. Thichanpiang, P.A. Okada, Applicability of a
634 colorimetric reverse transcription loop-mediated isothermal amplification (RT-LAMP) assay for
635 SARS-CoV-2 detection in high exposure risk setting, *Int. J. Infect. Dis.* 128 (2023) 285–289.
636 <https://doi.org/10.1016/j.ijid.2023.01.010>.
- 637 [57]I. Azmi, M.I. Faizan, R. Kumar, S. Raj Yadav, N. Chaudhary, D. Kumar Singh, R. Butola, A. Ganotra,
638 G. Datt Joshi, G. Deep Jhingan, J. Iqbal, M.C. Joshi, T. Ahmad, A Saliva-Based RNA Extraction-

- 639 Free Workflow Integrated With Cas13a for SARS-CoV-2 Detection, *Front. Cell. Infect. Microbiol.*
640 11 (2021). <https://www.frontiersin.org/articles/10.3389/fcimb.2021.632646> (accessed May 30,
641 2023).
- 642 [58]S. Wei, H. Suryawanshi, A. Djandji, E. Kohl, S. Morgan, E.A. Hod, S. Whittier, K. Roth, R. Yeh, J.C.
643 Alejaldre, E. Fleck, S. Ferrara, D. Hercz, D. Andrews, L. Lee, K.A. Hendershot, J. Goldstein, Y. Suh,
644 M. Mansukhani, Z. Williams, Field-deployable, rapid diagnostic testing of saliva for SARS-CoV-2,
645 *Sci. Rep.* 11 (2021) 5448. <https://doi.org/10.1038/s41598-021-84792-8>.
- 646 [59]M.A. Lalli, J.S. Langmade, X. Chen, C.C. Fronick, C.S. Sawyer, L.C. Burcea, M.N. Wilkinson, R.S.
647 Fulton, M. Heinz, W.J. Buchser, R.D. Head, R.D. Mitra, J. Milbrandt, Rapid and Extraction-Free
648 Detection of SARS-CoV-2 from Saliva by Colorimetric Reverse-Transcription Loop-Mediated
649 Isothermal Amplification, *Clin. Chem.* 67 (2021) 415–424.
650 <https://doi.org/10.1093/clinchem/hvaa267>.
- 651 [60]Real-time COVID-19 testing | Cue, (n.d.). <https://cuehealth.com/products/how-cue-detects-covid-19/>
652 (accessed September 19, 2023).
- 653 [61]Respiratory Health Test — POC rapid PCR device, Visby Med. (n.d.).
654 <https://www.visbymedical.com/respiratory-health-test/> (accessed September 19, 2023).
- 655 [62]ID NOW COVID-19 2.0, (n.d.). [https://www.globalpointofcare.abbott/us/en/product-details/id-now-](https://www.globalpointofcare.abbott/us/en/product-details/id-now-covid-19-us.html)
656 [covid-19-us.html](https://www.globalpointofcare.abbott/us/en/product-details/id-now-covid-19-us.html) (accessed September 19, 2023).
- 657 [63]Aptitude, (n.d.). <https://www.apitudemedical.com/product/metrix-covid-19-test> (accessed September
658 19, 2023).
- 659 [64]E.A. Phillips, T.J. Moehling, K.F.K. Ejendal, O.S. Hoilett, K.M. Byers, L.A. Basing, L.A. Jankowski,
660 J.B. Bennett, L.-K. Lin, L.A. Stanciu, J.C. Linnes, Microfluidic rapid and autonomous analytical
661 device (microRAAD) to detect HIV from whole blood samples, *Lab. Chip.* 19 (2019) 3375–3386.
662 <https://doi.org/10.1039/C9LC00506D>.
663
664
665

Table 1. Examples of NAATs for SARS-CoV-2 detection

Target gene	IAC target	Sample matrix	Limit of Detection	Clinical sensitivity (%)	Clinical Specificity (%)	Amplification method	Detection method	Reference
SARS-CoV-2 Nsp3 gene		Synthetic RNA	100 copies/reaction	N/A	N/A	RT-LAMP, WarmStart Colorimetric LAMP 2X Master Mix, Bst 3.0 DNA Polymerase, SuperScript IV Reverse Transcriptase	Leuco crystal violet colorimetric method	Park et al.[48]
SARS-CoV-2 ORF1ab, N genes		Synthetic RNA	10-50 copies/reaction	N/A	N/A	RT-LAMP, WarmStart RTX reverse transcriptase, Bst 2.0 DNA polymerase	LFA (Milenia Biotec)	Bhadra et al.[49]
SARS-CoV-2 N, E ORF1a genes	Beta-actin gene, run separately	Synthetic RNA	1-2 copies/μL in dual primer reaction	N/A	N/A	RT-LAMP, WarmStart Colorimetric RT-LAMP 2X Master Mix	Colorimetric assay	Zhang et al.[10]
SARS-CoV-2 N gene		Nasal swabs	100 copies/reaction	97.5	99.7	RT-LAMP, WarmStart 2X Master Mix	Colorimetric assay	Dao Thi et al.[50]
SARS-CoV-2 N gene		Nasal swabs	118.6 copies/reaction	94	90	RT-LAMP, WarmStart Bst 3.0 DNA Polymerase, WarmStartR RT, Q5 High-Fidelity DNA Polymerase	Colorimetric assay	Lu et al.[40]
SARS-CoV-2 N, S genes		Nasal swabs	5 copies/μL	95.4	84	Enhanced recombinase polymerase amplification (eRPA), RNase H, Superscript IV RT	LFA (Milenia Biotec)	Qian et al. ⁵¹
SARS-CoV-2 N gene		Nasal swabs	100 copies/reaction	100	98.7	RT-LAMP, WarmStart Colorimetric RT-LAMP 2X Master Mix	Colorimetric assay	Back et al.[52]
SARS-CoV-2 ORF1ab gene		Nasal swabs	20 copies/reaction	100	100	RT-LAMP, Bst DNA polymerase, AMV reverse transcriptase	Colorimetric assay	Yan et al.[53]
SARS-CoV-2 ORF1ab, N genes		Nasal swabs	90 copies/μL	71.4	100	RT-RPA Basic Kit with T7 Exo-assisted PNA recognition of RPA amplicon	LFA	Zheng at al.[54]
SARS-CoV-2 E, M, and N genes		Nasal Swabs	187 copies/reaction	100%	N/A	triple-target RT-LAMP (ttRT-LAMP)	Colorimetric assay	Zhang et al[55].
SARS-CoV-2 RdRp gene	RNase P gene, run separately	Nasal swabs	1,526.76 copies/mL	91.67%	100%	FastProofTM 30 min-TTR SARS-CoV-2 RT-LAMP Kit	Colorimetric assay	P. Nuchnoi, P. Piromtong, S. Siribal et al.[56]
SARS-CoV-2 N, ORF1a genes	Human actin B gene, run separately	Nasal swabs	25,000 copies/mL	87.5	100	RT-LAMP, WarmStart Colorimetric RT-LAMP 2X Master Mix	Colorimetric assay	Anahtar et al.[9]
SARS-CoV-2 N, E genes	RNase P gene, run separately	Nasal swabs	10 copies/μL	95	100	RT-LAMP, WarmStart DNA Polymerase, WarmStart RTx Reverse Transcriptase, LbCas12a	LFA (Milenia Biotec, TwistDx)	Broughton et al.[15]
SARS-CoV-2 ORF1ab gene	18S rRNA, run separately	Nasal swabs	1 genome copies /μL with image analysis	N/A	N/A	RT-LAMP, GspSSD 2.0 polymerase, AMV-RT	Intercalating agent SYTO82 (nucleic acid stain)	Garneret et al.[11]
SARS-CoV-2 N, ORF1a genes	RNase P gene, run separately	Nasal swabs	5 copies /reaction	97.4	100	RT-LAMP, WarmStart, Colorimetric WarmStart 2X Master Mix, Bsm polymerase	Colorimetric assay	Papadakis et al.[12]
SARS-CoV-2 N, S genes	RNase P gene, run separately	Nasal swabs and saliva	S gene primer: 10 copies/reaction, N gene primer: 25 copies/reaction	*Only show positive samples with 100% agreement		RT-LAMP, WarmStart LAMP master mix	End point fluorescence	Yaren et al.[14]
SARS-CoV-2 E/S genes		saliva	200 copies/reaction	98	100	RT-RPA, reverse transcriptase enzyme (EpiScript)	LFA (Milenia Biotec)	Azmi et al.[57]
SARS-CoV-2 N, RdRp, ORF1ab genes		Saliva	200 copies /μL saliva	97	100	RT-LAMP, WarmStart DNA Polymerase, WarmStart RTx Reverse Transcriptase	Colorimetric assay	Davidson et al.[42]
SARS-CoV-2 ORF1ab gene		Saliva	1.4 copies/μL	96.7	97.1	HP-LAMP, WarmStart Colorimetric LAMP 2X Master Mix	Colorimetric assay	Wei et al.[58]
SARS-CoV-2 ORF1ab, N genes		Saliva	100-200 copies/reaction	85	100	RT-LAMP, WarmStart Colorimetric LAMP 2X Master Mix	Colorimetric assay	Lalli[59] et al.
SARS-CoV-2 N gene	Proprietary	Nasal swabs	1.3 copies/μL	97.4	99.1	RT-LAMP	Results sent to smartphone through app	Cue's COVID-19 Diagnostic Test[60]
SARS-CoV-2 N, ORF1ab genes	B2M RNA	Nasal Swabs	100 copies/swab	93.2	98.9	PCR	Lateral flow strip on device	Visby Medical Respiratory Health Test[61]
SARS-CoV-2 RdRp Gene	Proprietary	Nasal Swab	500 copies/swab	93.3	98.5	Isothermal nucleic acid amplification technology	Result displayed by instrument	ID NOW™ COVID-19 2.0[62]
SARS-CoV-2 N, ORF-1 genes	Proprietary	Saliva, nasal swab	Swab: 2000 GE/swab Saliva: 20 GE/μL (GE = genome equivalent)	Swab: 96.7 Saliva:90.3	Swab: 99.0 Saliva: 99.3	Isothermal molecular amplification	Result displayed by device	Aptitude Matrix™ COVID-19 Test[63]
SARS-CoV-2 ORF1a gene	18S rRNA, one-pot duplex	Saliva	100 copies/μL	95	100	RT-LAMP, 2X WarmStart LAMP master mix	LFA (BioUstar)	This work

Table S1. RT-LAMP primer sets targeting the 18S rRNA (IAC) and the ORF1ab gene (SARS-CoV-2 target)

Human 18S rRNA target (GenBank: AL592188.60) Target Size: 225bp	
GTTCAAAGCAGGCCCGAGCCGCCTGGATACCGCAGCTAGGAATAATGGAATAGGACCGCGGTTCTATTTTGTGGTTTTTCGGAAGT GAGGCCATGATTAAGAGGGACGGCCGGGGGCATTTCGTATTGCGCCGCTAGAGGTGAAATTCCTTGGACCGGCGCAAGACGGACC AGAGCGAAAGCATTTCGCAAGAATGTTTTTCATTAATCAAGAACGAAAGTCGGAGG	
18S rRNA F3	GTTCAAAGCAGGCCCGAG
18S rRNA B3	CCTCCGACTTTCGTTCTTGA
18S rRNA FIP	TGGCCTCAGTTCGAAAACCAA-CCTGGATACCGCAGCTAGG
18S rRNA BIP	GGCATTTCGTATTGCGCCGCT-GGCAAATGCTTTCGCTCTG
18S rRNA LF-DigN	/5DigN /AGA ACC GCG GTC CTA TTC CAT TAT T
18S rRNA LB-Biotin	/5-Biosg/ ATT CCT TGG ACC GGC GCA AG

ORF1ab of SARS-CoV-2 target (GenBank: OQ691200.1) Target Size: 202bp	
TGGACCCCAAAAATCAGCGAAATGCACCCCGCATTACGTTTGGTGGACCCTCAGATTCAACTGGCAGTAACCAGAATGGAGAACGC AGTGGGGCTCGATCAAAACAACGTGCGCCCAAGGTTTACCCAATAATACTGCGTCTTGGTTCACCGCTCTCACTCAACATGGCAA GGAAGACCTTAAATTCCCTCGAGGACAAGGC	
SARS-CoV-2 F3	TGGACCCCAAAAATCAGCG
SARS-CoV-2 B3	GCCTTGTCTCTCGAGGGAAT
SARS-CoV-2 FIP	CCACTGCGTTCTCCATTCTGGT-AAATGCACCCCGCATTACG
SARS-CoV-2 BIP	CGCGATCAAAACAACGTGCGCCC-TTGCCATGTTGAGTGAGA
SARS-CoV-2 LF-FITC	/56-FAM/ GTTGAATCTGAGGGTCCACCA
SARS-CoV-2 LB-Biotin	/5Biosg/ACCCAATAATACTGCGTCTTGG

Table S2. LFIA analysis of RT-LAMP performed on 30 clinical samples with and without extraction. IAC and test line intensities of each of 3 replicates of RT-LAMP assays are shown. Intensity of greater than 0.02 or greater is considered positive by eye [64]. P represents positive. N represents negative. Sample ID 6 was the only sample that indicated discordant results between extracted and non-extracted samples.

Sample ID	The presence of IAC and test lines						IAC and test line intensities											
	Extracted samples			Non-extracted samples			Extracted samples			Non-extracted samples								
	IAC line	CoV-2 line	Result	IAC line	CoV-2 line	result	IAC			SARS-CoV-2			IAC			SARS-CoV-2		
						1	2	3	1	2	3	1	2	3	1	2	3	
1	Y	Y	P	Y	Y	faint P	0.123	0.115	0.108	0.021	0.018	0.017	0.099	0.099	0.087	0.010	0.019	0.016
2	Y	Y	P	Y	Y	P	0.097	0.077	0.050	0.078	0.083	0.063	0.123	0.089	0.121	0.036	0.053	0.017
3	Y	Y	P	Y	Y	P	0.065	0.088	0.084	0.088	0.101	0.065	0.117	0.104	0.145	0.050	0.045	0.027
4	Y	N	N	Y	N	N	0.110	0.116	0.109	-0.002	-0.002	-0.002	0.084	0.114	0.093	-0.001	-0.003	-0.002
5	Y	Y	P	Y	Y	P	0.078	0.090	0.072	0.097	0.143	0.109	0.102	0.082	0.066	0.037	0.084	0.082
6	Y	Y	P	Y	N	N	0.095	0.101	0.144	0.001	0.044	0.002	0.086	0.090	0.096	0.003	0.000	0.004
7	Y	Y	P	Y	Y	P	0.104	0.070	0.038	0.124	0.101	0.065	0.094	0.083	0.070	0.099	0.086	0.066
8	Y	N	N	Y	N	N	0.124	0.133	0.114	-0.002	-0.003	-0.001	0.103	0.049	0.097	-0.002	0.002	0.001
9	Y	Y	P	Y	Y	P	0.113	0.098	0.065	0.062	0.117	0.074	0.075	0.047	0.065	0.079	0.045	0.076
10	Y	Y	P	Y*	Y	P	0.047	0.047	0.057	0.160	0.104	0.100	0.009	0.007	0.009	0.137	0.101	0.100
11	Y	N	N	Y	N	N	0.126	0.115	0.123	0.001	-0.001	0.001	0.080	0.141	0.113	0.000	-0.001	-0.001
12	Y	Y	P	Y	Y	P	0.092	0.091	0.101	0.086	0.049	0.070	0.066	0.086	0.085	0.080	0.074	0.055
13	Y	Y	P	Y	Y	P	0.067	0.052	0.093	0.095	0.089	0.030	0.113	0.089	0.067	0.022	0.017	0.065
14	Y	Y	P	Y	Y	P	0.070	0.046	0.061	0.118	0.078	0.124	0.058	0.064	0.069	0.085	0.097	0.129
15	Y	Y	P	Y	Y	P	0.068	0.048	0.072	0.109	0.088	0.107	0.039	0.053	0.049	0.069	0.086	0.127
16	Y	Y	P	Y	Y	P	0.066	0.087	0.066	0.109	0.155	0.102	0.056	0.080	0.037	0.088	0.127	0.072
17	Y	Y	P	Y	Y	P	0.069	0.066	0.071	0.093	0.119	0.108	0.042	0.053	0.044	0.100	0.132	0.091
18	Y	Y	P	Y	Y	P	0.101	0.088	0.095	0.044	0.034	0.028	0.122	0.077	0.122	0.083	0.037	0.068

19	Y	Y	P	Y	Y	P	0.052	0.041	0.063	0.087	0.094	0.110	0.129	0.115	0.113	0.037	0.079	0.033
20	Y	N	N	Y	N	N	0.100	0.118	0.096	0.000	0.001	0.001	0.082	0.123	0.112	-0.003	0.001	0.000
21	Y	Y	P	Y	Y	P	0.099	0.089	0.098	0.019	0.014	0.016	0.120	0.145	0.128	0.033	0.038	0.047
22	Y	N	N	Y	N	N	0.075	0.113	0.127	0.000	-0.001	0.000	0.137	0.069	0.099	0.001	0.002	0.000
23	Y	N	N	Y	N	N	0.075	0.107	0.121	-0.001	-0.007	-0.002	0.087	0.101	0.096	-0.001	0.000	-0.002
24	Y	Y	P	Y	Y	P	0.111	0.129	0.111	0.010	0.019	0.013	0.115	0.123	0.112	0.039	0.032	0.026
25	Y	Y	P	Y	Y	P	0.061	0.058	0.063	0.098	0.088	0.075	0.074	0.053	0.081	0.095	0.117	0.110
26	Y	Y	P	Y	Y	P	0.081	0.078	0.090	0.078	0.064	0.070	0.131	0.115	0.122	0.062	0.046	0.048
27	Y	Y	P	Y	Y	P	0.079	0.079	0.079	0.124	0.089	0.095	0.085	0.079	0.072	0.081	0.092	0.080
28	Y	N	N	Y	N	N	0.135	0.110	0.115	0.002	0.001	-0.001	0.195	0.126	0.152	-0.004	-0.001	-0.001
29	Y	N	N	Y	N	N	0.119	0.138	0.117	0.000	-0.004	0.000	0.163	0.118	0.143	0.001	0.000	-0.003
30	Y	N	N	Y	N	N	0.130	0.100	0.123	-0.001	0.000	-0.001	0.148	0.141	0.165	-0.003	0.004	0.000

Table S3. Ct values of clinical sample ID 1-30. A positive result requires a sigmoidal amplification curve in the FAM channel with a Ct value of ≤ 37 , and a sigmoidal amplification curve in the VIC/HEX channel with a Ct value of ≤ 35 . A negative result is indicated by the absence of a sigmoidal amplification curve in the FAM channel with a Ct value of “0” or a sigmoidal amplification curve in the VIC/HEX channel with a Ct value of ≤ 35 . P represents positive. N represents negative.

Sample ID	Extracted samples				result
	BGI qPCR				
	FAM ct		VIC ct		
1	30.372	33.506	21.911	23.348	P
2	35.325	35.133	28.100	28.778	P
3	24.379	24.372	23.274	24.505	P
4	0	0	24.562	24.940	N
5	29.733	30.525	20.450	20.599	P
6	33.643	33.833	26.562	26.226	P
7	26.822	25.953	25.323	23.809	P
8	37.132	37.489	24.375	25.993	N
9	30.965	29.877	22.641	22.267	P
10	22.319	22.117	24.264	24.843	P
11	0	0	25.485	25.638	N
12	31.001	31.219	22.754	22.738	P
13	32.311	25.038	34.340	25.641	P
14	27.356	27.021	29.878	29.464	P
15	25.753	25.065	24.059	22.999	P
16	22.972	23.046	23.004	22.862	P
17	23.417	21.674	23.398	21.527	P
18	32.618	33.312	30.102	29.607	P
19	21.441	21.083	24.302	24.517	P
20	0.000	0.000	24.115	24.192	N
21	32.384	32.205	25.081	25.211	P
22	0	0	29.103	27.581	N
23	0	0	20.637	24.378	N
24	33.581	35.209	21.984	21.707	P
25	26.267	26.419	23.427	23.957	P
26	30.643	24.207	32.105	25.253	P
27	29.981	30.303	26.780	27.682	P
28	0	0	30.147	30.456	N
29	0	0	27.319	25.731	N
30	0	0	32.767	32.927	N

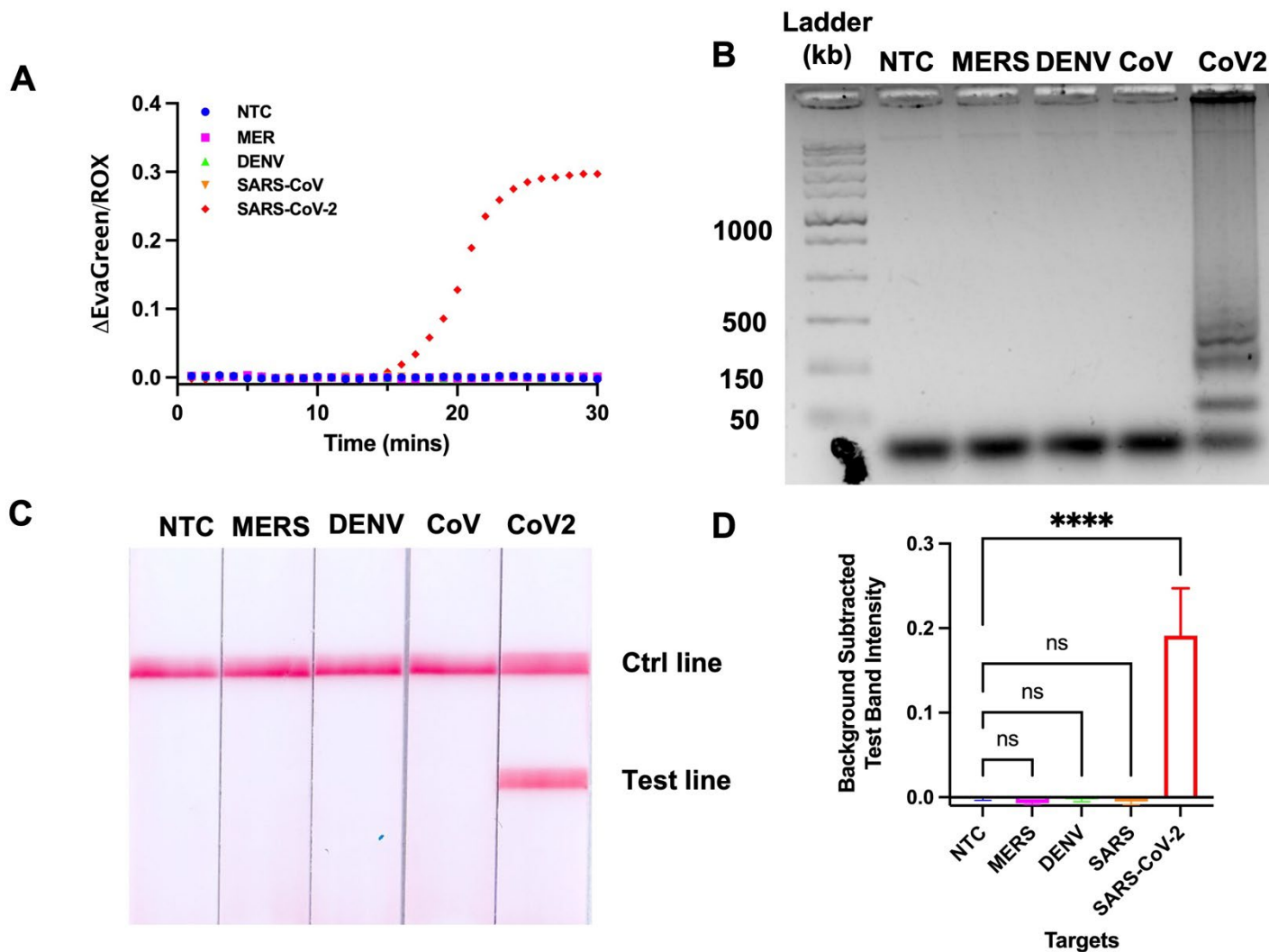


Figure S1. Analytical specificity of SARS-CoV-2 RT-LAMP assay against other viruses. (A) Amplification plot showed sigmoidal curve of SARS-CoV-2 template (B) Gel electrophoresis showed ladder pattern of amplified products of SARS-CoV-2 only. (C) The amplicons visualized on LFIA. Only reaction with SARS-CoV-2 generated test band. (D) corresponding test band intensity analysis. n = 3; **** indicates $p \leq 0.0001$

UCSC In-Silico PCR

No matches to `gttcaaagcaggccccgag cctccgacttctgttctga` in SARS-CoV-2 Jan. 2020 (NC_045512.2)

Primer Melting Temperatures

Forward: 61.9 C `gttcaaagcaggccccgag`

Reverse: 60.4 C `cctccgacttctgttctga`

The temperature calculations are done assuming 50 mM salt and 50 nM annealing oligo concentration. The code to calculate the melting temp comes from [Primer3](https://primer3.sourceforge.io/).

Figure S2. *In-silico* validation of 18S rRNA primer against SARS-CoV-2 genome.

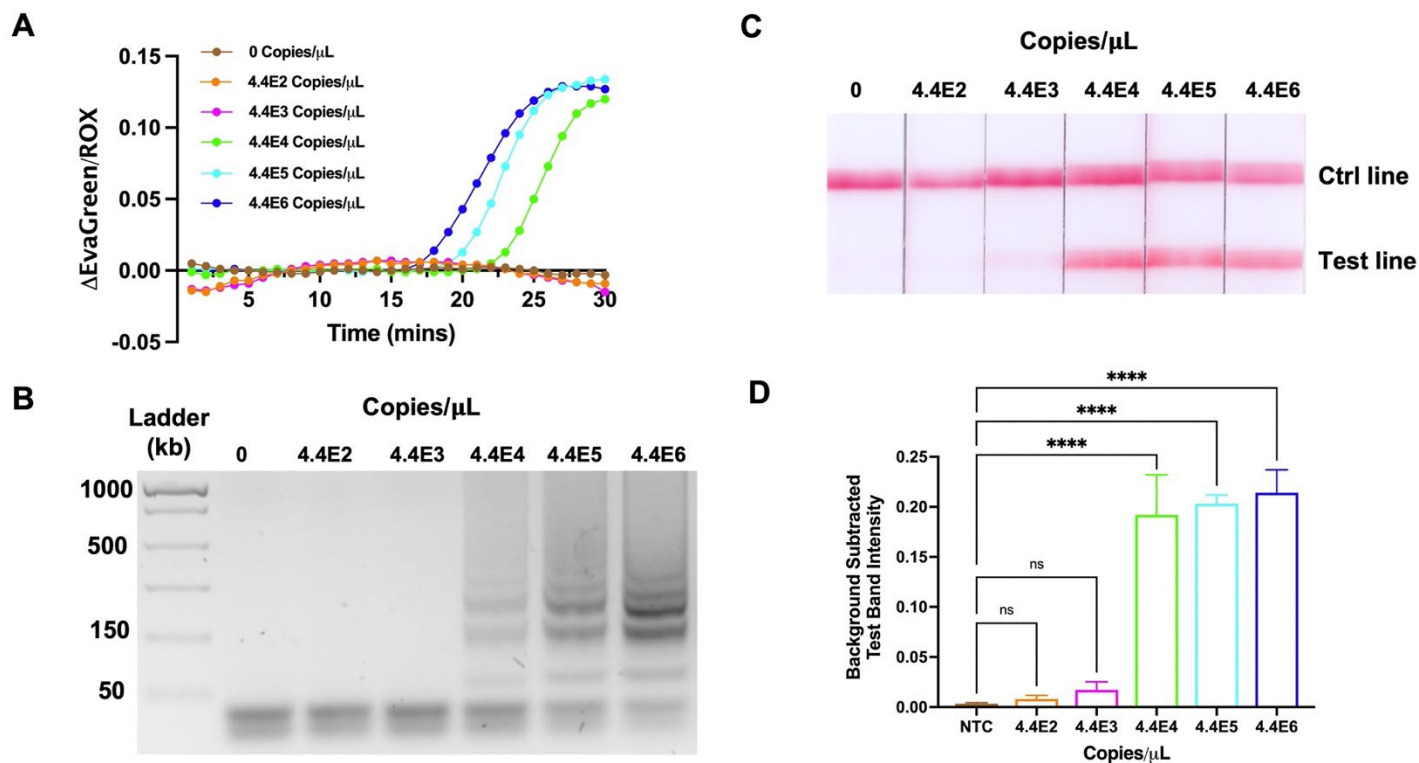
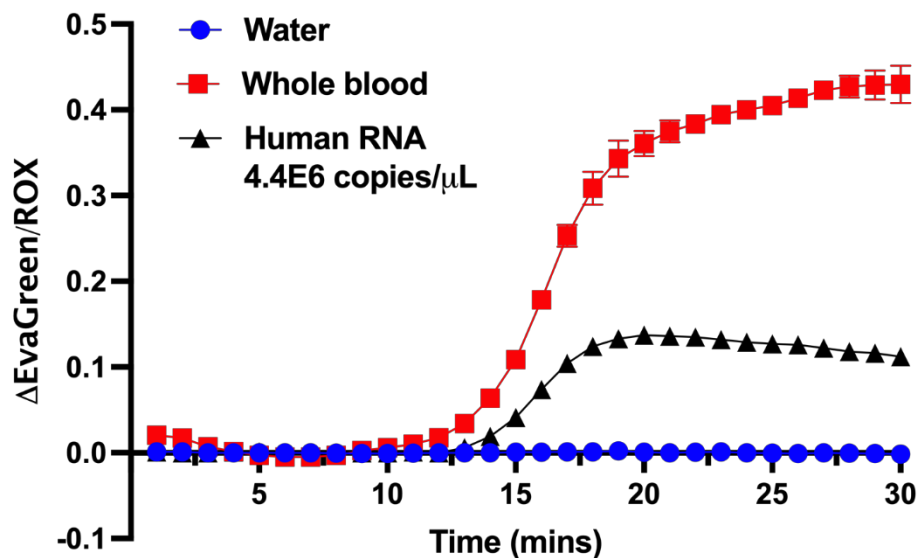


Figure S3. Figure S3. Analytical sensitivity 18S rRNA RT-LAMP assay. The amplification plot of 18S rRNA RT-LAMP using various concentration of human RNA control as templates (A). The corresponding gel electrophoresis analysis of 18S rRNA RT-LAMP amplicons (B). The LOD analysis on LFIA (C). The corresponding test band intensity analysis (D). n = 3; **** indicates $p \leq 0.0001$.



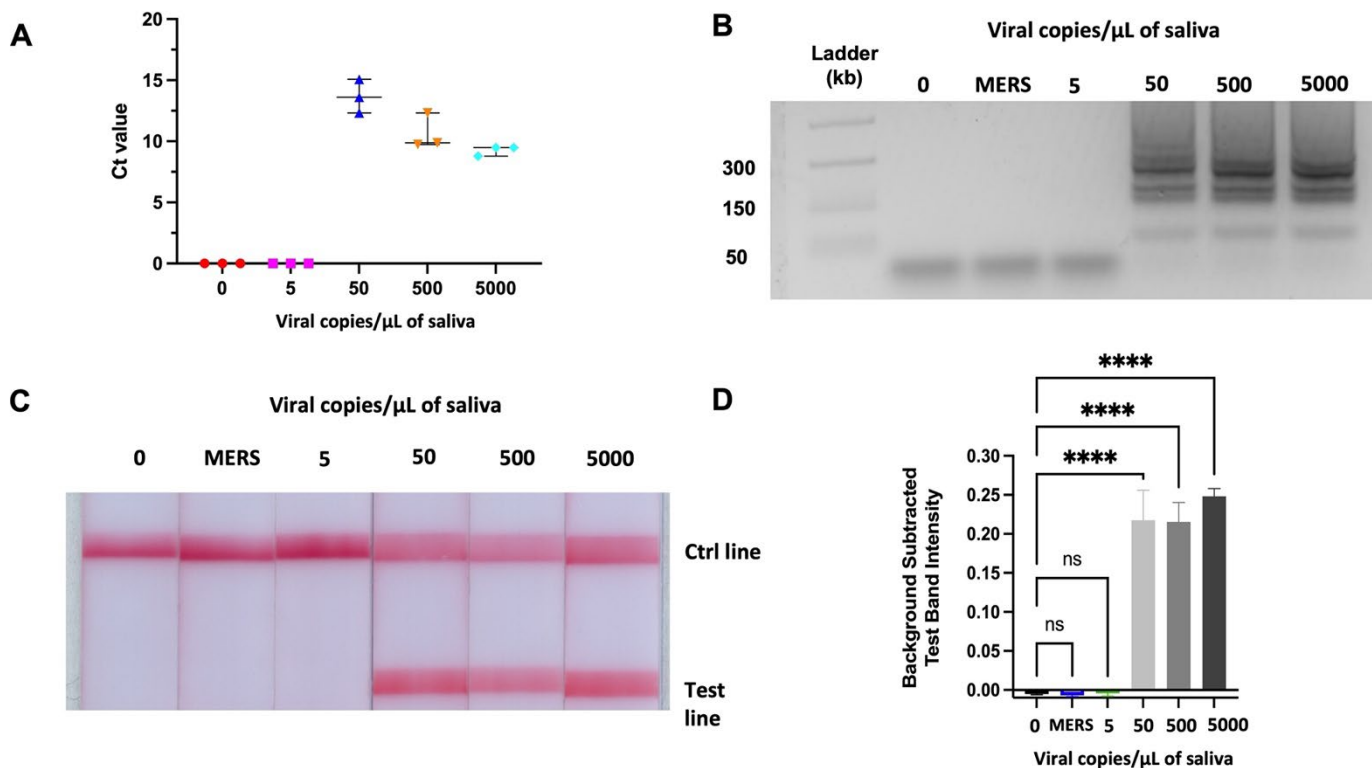


Figure S5. Analytical sensitivity of SARS-CoV-2 RT-LAMP assay in saliva with prior heat-treatment. RT-LAMP based detection of inactivated viral particles visualized on (A) gel electrophoresis (B) LFIA, and (C) corresponding test band intensity analysis. $n = 3$; **** indicates $p \leq 0.0001$.

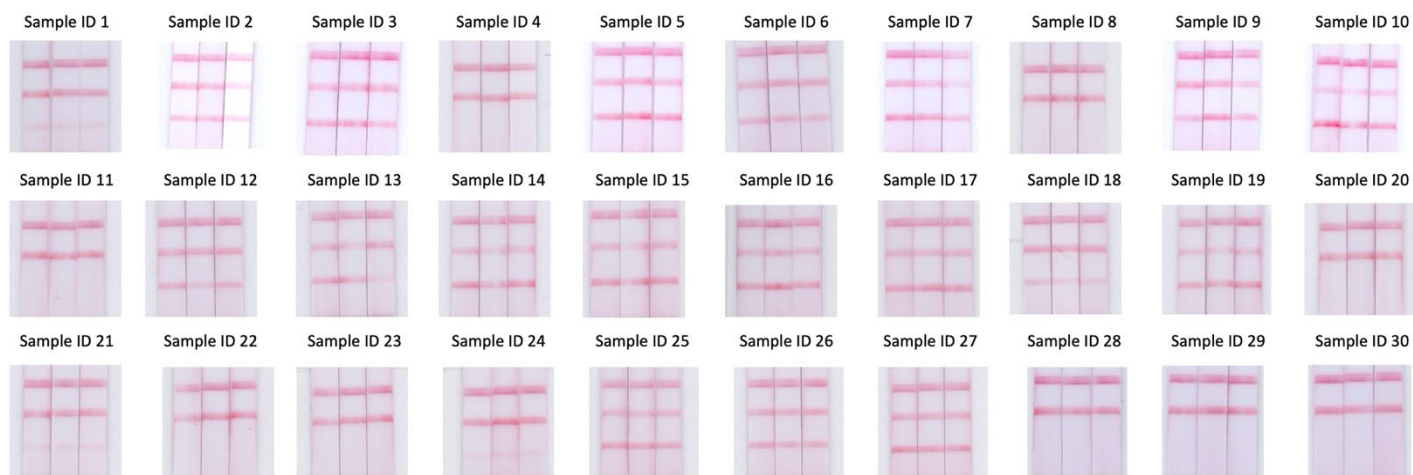


Figure S6. LFIA strips of extracted clinical samples, with the three lines representing “ctrl”, “IAC”, and test (from the top)

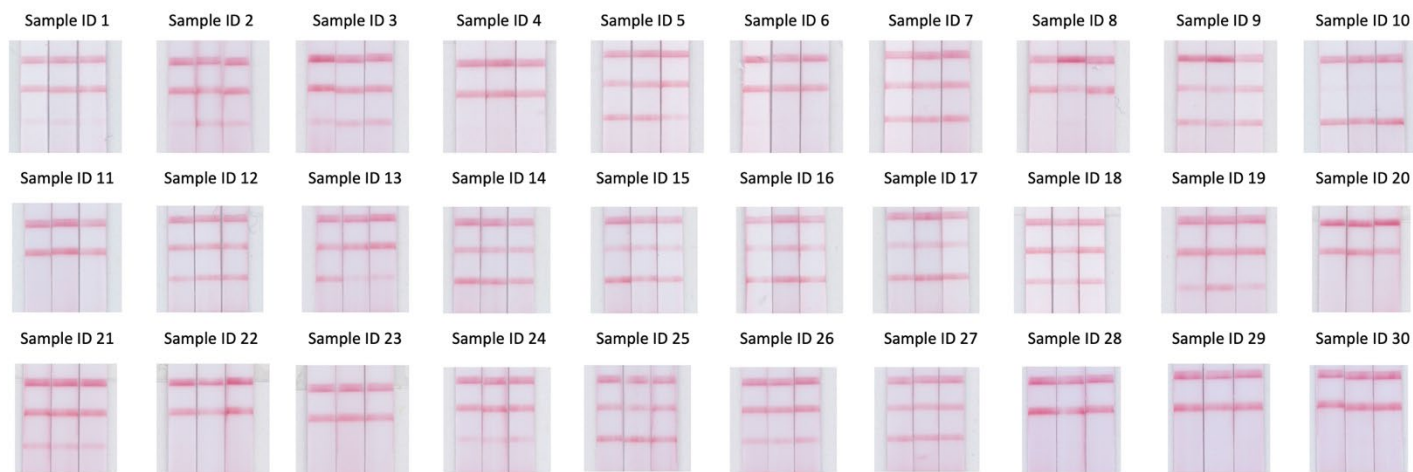


Figure S7. LFIA strips of non-extracted clinical samples